Neurophotonics

Neurophotonics.SPIEDigitalLibrary.org

Serotype-dependent transduction efficiencies of recombinant adeno-associated viral vectors in monkey neocortex

Annelies Gerits
Pascaline Vancraeyenest
Samme Vreysen
Marie-Eve Laramée
Annelies Michiels
Rik Gijsbers
Chris Van den Haute
Lieve Moons
Zeger Debyser
Veerle Baekelandt
Lutgarde Arckens
Wim Vanduffel

SPIE.

Neurophotonics 2(3), 031209 (Jul–Sep 2015)

Serotype-dependent transduction efficiencies of recombinant adeno-associated viral vectors in monkey neocortex

Annelies Gerits,[a,†] Pascaline Vancraeyenest,[a,†] Samme Vreysen,[b] Marie-Eve Laramée,[b] Annelies Michiels,[c,d] Rik Gijsbers,[d,e] Chris Van den Haute,[c,d] Lieve Moons,[f] Zeger Debyser,[e] Veerle Baekelandt,[c] Lutgarde Arckens,[b] and Wim Vanduffel[a,g,h,*]

[a]KU Leuven, Laboratory of Neuro- and Psychophysiology, Department of Neurosciences, O&N2 Herestraat 49 bus 10.21, 3000 Leuven, Belgium
[b]KU Leuven, Laboratory of Neuroplasticity and Neuroproteomics, Faculty of Science, Naamsestraat 59, 3000 Leuven, Belgium
[c]KU Leuven, Laboratory for Neurobiology and Gene Therapy, Department of Neurosciences, Kapucijnenvoer 33, VCTB +5, 3000 Leuven, Belgium
[d]KU Leuven, Leuven Viral Vector Core, Kapucijnenvoer 33, VCTB +5, 3000 Leuven, Belgium
[e]KU Leuven, Laboratory of Molecular Virology and Gene Therapy, Department of Neurosciences, Kapucijnenvoer 33, VCTB +5, 3000 Leuven, Flanders, Belgium
[f]KU Leuven, Laboratory of Neural Circuit Development and Regeneration, Faculty of Science, Naamsestraat 61, 3000 Leuven, Belgium
[g]Massachusetts General Hospital, Athinoula A. Martinos Center for Biomedical Imaging, 149 13th street, Charlestown, Massachusetts 02129, United States
[h]Harvard Medical School, Department of Radiology, 149 13th street, Charlestown, Massachusetts 02129, United States

Abstract. Viral vector-mediated expression of genes (e.g., coding for opsins and designer receptors) has grown increasingly popular. Cell-type specific expression is achieved by altering viral vector tropism through cross-packaging or by cell-specific promoters driving gene expression. Detailed information about transduction properties of most recombinant adeno-associated viral vector (rAAV) serotypes in macaque cortex is gradually becoming available. Here, we compare transduction efficiencies and expression patterns of reporter genes in two macaque neocortical areas employing different rAAV serotypes and promoters. A short version of the calmodulin-kinase-II (CaMKIIα0.4) promoter resulted in reporter gene expression in cortical neurons for all tested rAAVs, albeit with different efficiencies for spread: rAAV2/5>>rAAV2/7>rAAV2/8>rAAV2/9>>rAAV2/1 and proportion of transduced cells: rAAV2/1>rAAV2/5>rAAV2/7=rAAV2/9>rAAV2/8. In contrast to rodent studies, the cytomegalovirus (CMV) promoter appeared least efficient in macaque cortex. The human synapsin-1 promoter preceded by the CMV enhancer (enhSyn1) produced homogeneous reporter gene expression across all layers, while two variants of the CaMKIIα promoter resulted in different laminar transduction patterns and cell specificities. Finally, differences in expression patterns were observed when the same viral vector was injected in two neocortical areas. Our results corroborate previous findings that reporter-gene expression patterns and efficiency of rAAV transduction depend on serotype, promoter, cortical layer, and area. [DOI: 10.1117/1.NPh.2.3.031209]

Keywords: promoters; histology; monkey; optogenetics; gene transfer; cell-specific expression.

Paper 15010SSPR received Feb. 4, 2015; accepted for publication Aug. 25, 2015; published online Oct. 1, 2015.

1 Introduction

For more than three decades, viral vectors have been used extensively to deliver genetic material into specific subsets of cells throughout the body, with the ultimate goal of human gene therapy.[1–5] To this end, recombinant viral vectors containing genes-of-interest and free of replication-essential elements have been bioengineered. Presently, such viral vectors are also widely used in basic biomedical research to express proteins in well-defined cell types.[6]

In neuroscience, several methods have recently been introduced to control neural activity with unprecedented specificity. Methods such as optogenetics,[7–11] "designer receptors exclusively activated by designer drugs" (in short, DREADD) [12–14] and the double-infection technique (DIT),[15,16] rely mainly on viral vectors to introduce genes encoding light-sensitive proteins (opsins), artificial receptors (DREADD), or neurotoxins (DIT) into neurons. Transduction of specific subsets of cells (i.e., tropism) is inherent to the viral vector used and depends on the interaction between viral vector envelope/capsid and receptors on the cell membrane. Subsequent reporter or transgene expression depends on the potency of the heterologous promoter and the availability of transcription factors (TFs) for this promoter in the targeted cell (cell specificity).[17] Despite the abundant use of viral vectors, state-of-the-art neuroscience and clinical studies have exposed potential challenges. These include cross-species variation in vector tissue tropism and gene transfer efficiency, pre-existing humoral immunity to capsids, and vector dose-dependent toxicity in animal models and patients. Detailed information about the transduction characteristics of such vector systems in macaque neocortex, however, is only sparsely available.[18] This is particularly an issue considering the increasing popularity of viral vectors in nonhuman primate research.

The most frequently used viral expression systems are developed from adenoviruses, adeno-associated virus (AAV), herpes simplex virus, gamma retroviruses and lentiviruses (LV; subclass

*Address all correspondence to: Wim Vanduffel, E-mail: wim@nmr.mgh.harvard.edu

†These authors contributed equally to the manuscript.

of retroviruses), each having their particular advantages and limitations.[1,19] AAV and LV are most often used in the central nervous system (CNS) since they are relatively easy to produce and evoke minimal immune responses.[17,19] The packing capacity of AAV is low compared to LV, and genes delivered using AAV vectors do remain episomal in the transduced cell. Although LVs showed long-lasting expression[2,20] and were clinically successful in several primate studies,[21,22] AAV is considered to be more appealing for transgene expression in CNS. AAV is small (20 to 25 nm), nonenveloped, single-stranded DNA parvoviruses.[23] They are known for their efficient neuronal (NeuN) transduction, long-lasting transgene expression (up to 2 years in rodents and 6 years in primates) and safety profile (no integration in host-cell genome).[3,24–28] In addition, they can transduce both dividing and nondividing cells. The best-characterized AAV serotype, first cloned into bacterial plasmids, is AAV serotype 2 carrying an AAV2-derived genome (AAV2/2).[29] Through cross-packaging, AAV2-based genomes can be packaged in alternative AAV serotypes (e.g., rAAV2/5), which yields higher transduction efficiencies than AAV2/2. AAV-based vectors are currently the most widely used for preclinical research, due to favorable characteristics such as higher transduction efficiencies and greater dispersion.[30–32] Unfortunately, the latter properties are species specific and even brain region specific.[30,33] Moreover, information about transduction and expression properties obtained in rodents does not always translate to primates.[34–38] In macaque monkeys, a comparison between the transduction properties of different rAAVs in subcortical structures, including the substantia nigra, striatum,[39,40] and basal ganglia,[41] revealed that rAAV2/1 and rAAV2/5 were most efficient when under the control of a synthetic chicken ß-actin promoter. In addition, another study of Sanchez et al.[40] revealed a three- to fourfold higher efficiency of rAAV2/8 compared to rAAV2/1, 2/2, and 2/5 when using a cytomegalovirus (CMV) promoter. Optogenetic studies in macaques confirmed that viral vector transduction in cortex is heterogenous across cortical layers.[35,42,43] Recently, an exhaustive comparison of transduction efficiencies of various recombinant adeno-associated viral vector (rAAV) serotypes and promoters in marmoset, mouse, and macaque neocortex again revealed distinct transduction patterns depending on the serotype and promoter used in the viral vector.[18] Serotype rAAV2 showed a smaller spread compared to rAAV1, 5, 8, and 9, while constructs with the SynI promoter showed higher transgene expression in layers 3 and 5 compared to CaMKII-constructs.

Therefore, to optimize future optogenetic, DREADD, and DIT studies in macaque monkeys and to extend the results obtained by Watakabe et al.,[18] we determined the transduction patterns of several rAAV serotypes using the CMV, two variations of the CaMKII, and the enhSyn1 promoters in macaque cortex. Specifically, we investigated the efficiencies, laminar expression patterns, spread, cell specificities and potential antero- and/or retrograde projection properties of 12 different rAAV vector/promoter combinations injected into primary visual and prefrontal cortex of rhesus monkeys, using immunohistochemical evaluation of the reporter genes.

2 Materials and Methods

2.1 *Subjects*

Four hemispheres from the forebrains of two adult male rhesus monkeys (*Macaca mulatta*) were used in this study (M10: 6.2 kg and M37: 6.5 kg). Prior to these terminal experiments, both monkeys had participated in a series of electrophysiological and/or contrast-agent enhanced functional magnetic resonance imaging experiments unrelated to the present study.[44] All experimental procedures were approved by the regulations of the biosafety and ethical committees at KU Leuven and strictly adhered to the guidelines of the National Institutes of Health and the European guidelines for the care and use of laboratory animals.

2.2 *Vector Constructs*

The recombinant AAV2 vectors used in this study were packaged in AAV1, 5, 7, 8, 9 capsids (referred to as rAAV2/1, 2/5, 2/7, 2/8 and 2/9; Table 1). Expression of enhanced green fluorescent protein (EGFP) or membrane localized cherry red fluorescent protein (mCherry) was under the control of one of four promoters: human CMV, human enhSyn1, Mus musculus CaMKIIα0.4, or Mus musculus CaMKIIα1.3. Human enhSyn1 promoter was polymerase chain reaction (PCR) amplified from a plasmid provided by Hioki et al.[45] using ATTCTAGATAGTTA TTAATAGTAATCAATTACGGGG as forward and AGGAT CCCGCCGCAGCGCAG as reverse primer. The MmCa MKIIα1.3 promoter was PCR amplified from plasmid 20944 (addgene) using following primers: Fw—AAAGCTAGC CATTATGGCCTTAGGTCACTTCAT and Rev— AAAA GCGCTGATATCCCGCTGCCCCCAGAACTAGGGGC. The MmCaMKIIα0.4 fragment was amplified with—AAAGC TAGCACTTGTGGACTAAGTTTGTTCACATCCC—as forward and—AAAAGCGCTGATATCGCTGCCCCCAGAACT AGGGGCCACTCG—as reverse primer. These PCR fragments were ligated in the AAV transfer plasmid using XbaI and BamHI for enhSyn1 and NheI and Eco47 III for MmCaMKIIα after the hCMV promoter was cut out.

All vector constructs were generated by the Viral Vector Core at KU Leuven according to published procedures.[32] Briefly, serum-free rAAV production was performed by triple transient transfection of HEK 293T cells (ATCC, Manassas, Virginia) using the AAV transfer plasmids, AAV rep/cap (2/1, 2/5, 2/7, 2/8, or 2/9) and pAd.DELTA.F6 plasmid in the ratio of 1:1:1 using polyethylenimine. The supernatant was harvested 5 days after transient transfection, concentrated using tangential flow filtration, and purified using an iodixanol step gradient. Gradient fractions were collected in 250 μl aliquots and fractions with refraction indices between 1.39 and 1.42 were pooled. The iodixanol of the pooled fractions was exchanged five times with phosphate-buffered saline (PBS), in a Vivaspin 6 (PES, 100,000 MWCO, Sartorius AG, Goettingen, Germany). The resulting concentrated rAAV was aliquoted and stored at −80°C.

Genomic titers that were determined as genomic copy numbers of the respective rAAV preparations were evaluated by TaqMan-based quantitative PCR analysis using a primer probe set for the polyA sequence (primer sequences, 5′-TCTAGTTGCCAGCCATCTGTTGT-3′ and 5′-TGGGAGTGG CACCTTCCA-3′; probe sequence, 5′-TCCCCCGTGCCTT CCTTGACC–3′). Genome copies obtained for the different productions ranged from 4.0 × 10e11 to 4.8 × 10e12 genome copies/ml (Table 1).

The functional titers of rAAV2/7—CaMKIIα 0.4 and rAAV2/7—CaMKIIα 1.3 were determined as described earlier.[46] Briefly, 75.000 HEK-293T cells were incubated with a serial dilution of the respective rAAV vectors for 72 h. Following transduction, cells were washed, trypsinized, and the cell pellet was washed three more times with PBS. About 100 ng of genomic DNA

Table 1 Overview of injected viral vectors in M10 and M37. The short solid lines separate the different injection sessions. Identical serotype/promoter injections in M10 and M37 are labelled in bold.

		Serotype	Promoter	FP	Titer (E12)	Survival time	Region	Hemisphere
M10	**A**	**rAAV2/7**	**hCMV**	EGFP	1.9	29 d	V1	R
	B	**rAAV2/7**	**MmCaMKIIα0.4**	EGFP	2.6	29 d	V1	R
	C	rAAV2/5	hCMV	EGFP	0.4	29 d	V1	R
	D	**rAAV2/8**	**hCMV**	EGFP	2.6	78 d	V1	L
	E	**rAAV2/9**	**hCMV**	EGFP	3.2	78 d	V1	L
	F	**rAAV2/7**	**MmCaMKIIα1.3**	EGFP	2.6	78 d	V1	L
M37	G	rAAV2/1	hCMV	EGFP	1.1	93 d	DLPC	R
	H	**rAAV2/8**	**hCMV**	EGFP	1.9	93 d	DLPC	R
	I	**rAAV2/9**	**hCMV**	EGFP	1.2	93 d	DLPC	R
	J	**rAAV2/7**	**MmCaMKIIα0.4**	EGFP	2.6	93 d	DLPC	R
	K	rAAV2/1	MmCaMKIIα0.4	EGFP	1.0	52 d	V1	L
	L	rAAV2/5	MmCaMKIIα0.4	mCherry	4.8	52 d	V1	L
	M	**rAAV2/8**	**MmCaMKIIα0.4**	EGFP	2.8	52 d	V1	L
	N	**rAAV2/9**	**MmCaMKIIα0.4**	mCherry	3.1	52 d	V1	L
	O	**rAAV2/7**	**MmCaMKIIα1.3**	EGFP	3.0	52 d	V1	L
	P	**rAAV2/7**	**hCMV**	EGFP	1.5	29 d	V1	R
	Q	rAAV2/7	hCMV(en)hSyn	mCherry	1.3	29 d	V1	R
	R	**rAAV2/7**	**MmCaMKIIα0.4**	EGFP	3.1	29 d	V1	R
	S	**rAAV2/7**	**MmCaMKIIα1.3**	mCherry	2.1	29 d	V1	R

Note: FP, fluorescent protein; CMV, cytomegalovirus promoter; CaMKIIα, α-calcium/calmodulin-dependent protein kinase II promoter; enhSyn1, CMV enhanced human Synapsin-1 promoter; promoter size sequence: 0.4 and 1.3 kb; rAAV, recombinant adeno-associated viral vector; EGFP, enhanced green fluorescent protein; d, days; DLPC, dorsolateral prefrontal cortex; V1, primary visual cortex.

was used for the determination of the rAAV genomic copies using a real-time PCR, as described earlier.[33] Each dilution of the viral vectors was used three times and this experiment was done in two different assays.

A univariate general linear model test was performed with SPSS v16.0 for Windows to compare the effects of the dilution and promoter sequence (CaMKIIα 0.4 or CaMKIIα 1.3) on the functional titers, with the assay number as a cofactor. Bonferroni *posthoc* tests were performed to determine specific differences between the groups. The significance level was set to $p < 0.05$ for all statistical analyses.

2.3 *Vector Injections*

For the cortical injections of the vector, monkeys were first sedated with Domitor and Ketalar (50 mg/kg, intramuscular, Pfizer) and anesthetized with isoflurane (±1.2%). Postoperatively, the animals were treated with analgesics (Contramal, i.m.) and antibiotics (Kefzol, i.m). Five separate series of injections were performed, two in M10 (separated by 7 weeks) and three in M37 (separated by 6 and 3 weeks, respectively; Table 1). The time between the last series of injections and the perfusion was 4 weeks for both subjects. Four series of injections targeted area V1 and one series prefrontal cortex (area 46). Craniotomies were performed above area V1 (M10 and M37) and above frontal cortex (only in M37). After incising and partially retracting the dura mater, viral vectors were injected using a Nanoject II Auto-Nanoliter Injector (Drummond Scientific Company) attached to a custom-built micromanipulator with three translational degrees of freedom (XYZ-manipulator). Next, the vector was loaded into pulled glass micropipettes (outer diameter of 50 μm). At each location, a total volume of 920 nL was injected at 10 equally distributed positions between the gray-white matter boundary and the pial surface (total distance of 1.8 mm) with a series of four injections of 23 nL each at a single position every 10 s and applying an interval of 2 min between consecutive vertical positions [Fig. 1(a)].

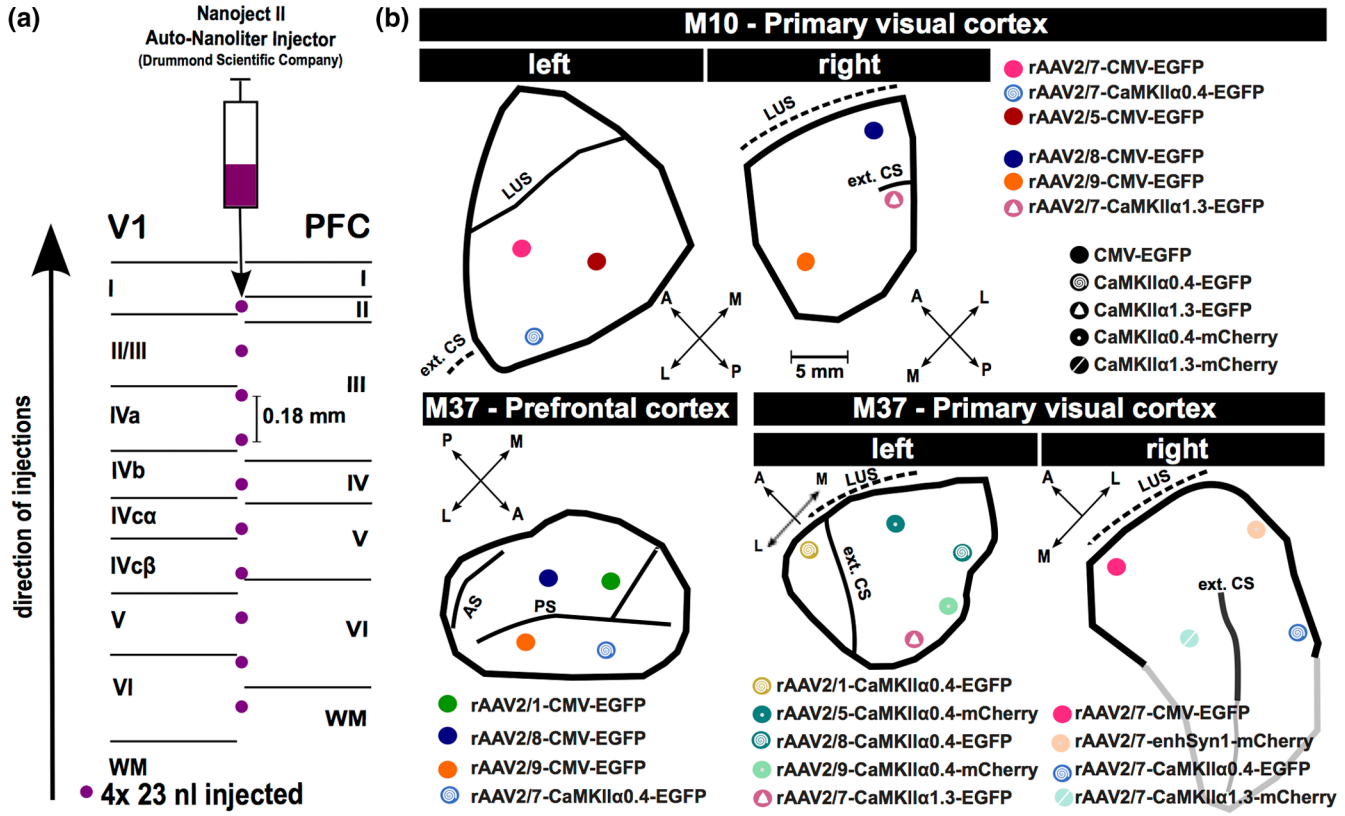

Fig. 1 Injection procedure across cortical layers. (a) Schematic representation of injection procedure. In total, 920 nL of each vector was injected across 10 equidistant positions in depth (indicated with purple dots), with a spacing of 0.18 mm perpendicular to the cortex. (b) Cortical locations of all injection sites within each craniotomy with an indication of the neighboring sulci that were visible during surgery (left and right V1 for M10, left and right V1 and right 46a for M37). Abbreviations: A, anterior; AS, arcuate sulcus; Ext. CS, external calcarine sulcus; L, lateral; LUS, lunate sulcus; M, medial; P, posterior; PS, principale sulcus; wm, white matter.

To match the vector to its corresponding position, a photo was taken and distances to main anatomical landmarks (e.g., sulci) were measured at each injection site [see Fig. 1(b) for schematic overview of the injection sites relative to sulci and the border of the respective craniotomies]. Once the viral vector injections were completed at a particular site, the dura mater was sutured, the original bone was used to cover the craniotomy, and the skin was closed over the bone flap.

2.4 *Perfusion*

Four weeks after the final injection series, both monkeys were deeply anesthetized (ketalar, 50 mg/kg, intramuscular, Pfizer) and euthanized using an overdose of pentobarbital (intravenous, 30 mg/kg, Sigma). The animal was then transcardially perfused using isotonic saline [9% NaCl in 0.1 M phosphate buffer, pH 7.4 (PB)], followed by 3.5% paraformaldehyde in PB solution and finally with 5% glycerol in PB for cryoprotection. Subsequently, the brain was removed from the skull, cut in six to eight pieces and stored for 3 days in 10% and 3 days in 20% glycerol–PB solution. Tissue pieces were quickly frozen in 2-methylbutane (Merck) at −30 to −40°C, stored at −80°C, and sectioned with a cryostat at −30°C (50-μm-thick coronal sections). The sections were stored as free-floating sections in 0.01% sodium azide containing PBS buffer (0.15 M, pH 7.4) at 4°C until further processing.

2.5 *Histology*

Since the pipette tracks caused by the injections were not visible in unstained sections, a series of cryosections (every 200 μm) were mounted onto glass plates. Cresyl violet and immunohistochemical fluorescent protein (FP) staining were then performed on two different series. Based upon the FP-staining, the injection sites could be determined as the sections with the highest proportion of FP-labeled cells across all layers. Parvalbumin (PV) and NeuN stainings were additionally performed on a series of adjacent sections to calculate the percentage of FP+ cells compared to the total number of neurons (NeuN) and to ascertain cell-type specificity (PV).

2.5.1 *Cresyl violet staining*

Free-floating sections (50 μm) were mounted onto poly-L-lysine-coated (Sigma-Aldrich) glass slides and kept at 37°C for 1 day (Heraeus, type B5050). Cresyl violet staining was then performed according to standard methods to delineate areal borders and cortical layers delineation, as previously described.[47,48]

2.5.2 *Immunohistochemistry*

Table 2 summarizes all details concerning antibodies, dilutions, and buffers used in immunohistochemistry. All free-floating sections (50 μm) were washed twice in 1× tris-buffered saline

Table 2 Overview of primary and secondary antibodies used in immunohistochemical staining.

Single Staining

FP	Primair antibody	Buffer	(1: X)	Secundair antibody (in TNB)	(1: X)
G	Mm anti-parvalbumin (Swant)	TNB	60000	Biotinylated GAM (polyclonal; invitrogen)	500
G	Rb anti-EGFP (Lab. NB-GT)	TNB	10000	GAR IgG, AF594 (PC, ab150088; Abcam)	250
G	Mm anti-parvalbumin (Swant)	TNB	60000	GAM IgG, AF594 (PC, ab150120, Abcam)	250
R	Rb anti-RFP (ab 600-401-379; Rockland)	TNB	5000	GAR IgG, AF488 (PC, ab150085, Abcam)	250

Double Staining

FP	Primair antibody	Buffer	(1: X)	Secundair antibody (in TNB)	(1: X)
G	Rb anti-EGFP (Lab. NB-GT)	PBS*	10000	GAR IgG, AF488 (PC, ab150085, Abcam)	250
G	Mm anti-NeuN (MAB377, Merck)	PBS*	200	GAM IgG, AF594 (PC, ab150120, Abcam)	250
G	Rb anti-EGFP (Lab. NB-GT)	PBS*	10000	GAR IgG, AF488 (PC, ab150085, Abcam)	250
G	Mm anti-NeuN (MAB377, Merck)	PBS*	200	GAM IgG, AF594 (PC, ab150120, Abcam)	250
R	Rb anti-RFP (ab 600-401-379; Rockland)	PBS*	5000	GAR IgG, AF594 (PC, ab150088, Abcam)	250
R	Mm anti-NeuN (MAB377, Merck)	PBS*	200	GAM IgG, AF488 (PC, ab150117, Abcam)	250

Note: Mm, mouse; PBS*, phosphate-buffered saline 0.1%Triton-X100 10%PIG; PC, Polyclonal; R, mCherry-RFP; Rb, Rabbit; Ab, Abcam, Cambridge, United Kingdom; G, EGFP; Lab. NB-GT, Laboratory of Neurobiology and Gene Therapy, KU Leuven, Belgium; Merck, Merck Milipore, Darmstadt, Germany; invitroge, (Invitrogen Corporation, Carlsbad, California; Rb, Rabbit; RL, Rockland Immunochemicals Inc., Gilbertsville, Pennsylvania; Swant, Swant swiss antibodies, Switzerland; TNB, tris-NaCl-blocking buffer, 1× TBS, 0.5% blocking buffer.

or 1× PBS 0.1% TRITONX-100 (for NeuN) (10 min) and then pretreated for 45 min with preimmune goat serum [(PIG); 1:5 dilution]. For NeuN staining, an additional pretreatment for 20 min in a methanol 0.3% peroxide solution preceded the PIG incubation step. After overnight, incubation at 4°C with primary antibody (Table 2) sections was rinsed in wash buffer. The tissue was then incubated at room temperature (RT) for 2 h with appropriate secondary antibodies (Table 2). For biotinylated secondary antibodies, slices were additionally washed (3×10 min) and incubated with streptavidin-Cy5 at RT for 2 h (1:500, invitrogen). Following 3×10 min washing steps in wash buffer, the sections were rinsed quickly in aqua destillata and sections were incubated for 30 min in 4′,6-diamidino-2-phenylindole (2 μl/100 ml 0.1 M PBS). Finally, the floating slices were mounted onto gelatin-bloom coated slides (0.05% gelatin bloom solution, type 2, sigma) and cover-slipped with mowiol mounting medium for examination by fluorescence microscopy.

2.6 *Image Acquisition*

All (immuno-)histochemically stained sections were imaged (10×, 20×, and 40× dry lenses) with a Zeiss Axio-Imager microscope equipped with Zeiss CCD Axiocam black and white and color cameras (MRc3 and MRc5, respectively). Fluorescent photographs for semiquantification were additionally acquired with an Olympus Fluoview FV1000 inverted confocal microscope (4×, 10×, and 20× objectives) and using the Olympus Fluoview acquisition software 3.0a. After defining the region of interest, the software divided this region into four to six sections and a z-stack (to cover the 50-μm-thick slice) was acquired.

2.7 *Proportion of Transduced Neurons*

To determine the fraction of all neurons and inhibitory-specific neurons transduced for each vector, confocal images of the NeuN stainings and PV stainings were taken. To approximately define the proportion of colocalizing cells, a semiquantitative analysis (i.e., manual quantification in one section) was performed. Therefore, images were first cropped to the preferred size. Layers were then defined based on NeuN stainings and compared to neighboring CV-stained slices. Afterward, the overlap with fluorescently labeled neurons was manually scored and quantified across the different cortical layers for each image, as described in Diester et al.,[35] using ImageJ (image processing and analysis in Java, National Institute of Health).

When a percentage of transduced neurons is mentioned in the results, these numbers were obtained from sections adjacent to the injection site. The percentage was calculated as the number of colocalized FP+ and NeuN+ cells divided by the total number of NeuN+ cells multiplied by 100. The numbers representing the spread are based on the maximal distance from the injection site at which FP+ cells were found across the cortical surface. The anterior–posterior (A-P) axis is always mentioned first followed by the spread along the lateral–medial (L-M) axis.

3 Results

We injected a series of rAAV vectors into two cortical brain regions of both hemispheres in two monkeys (M10 and M37) to determine their transduction efficiency and apparent distribution pattern, as evaluated by reporter gene expression (Fig. 1). In M10, serotypes rAAV2/5, 2/7, 2/8 and 2/9 were

injected into left and right area V1. FP-expression was driven by i) a constitutive CMV promoter (rAAV2/5, 2/7, 2/8 and 2/9), ii) a long, or iii) short version of the excitatory cell type-specific CaMKIIα promoter (rAAV2/7). The long version of the CaMKIIα promoter (1.3 kb; CaMKIIα1.3) has been used previously and was found to transduce excitatory cells in several species including mouse, rat and monkey.[43,49–51] Additionally, a shorter CaMKIIα promoter (0.4 kb; CaMKIIα0.4)[52] was constructed to facilitate packaging of larger genes (e.g., opsins) in future experiments.

In the second monkey (M37), three injection sessions were carried out. In the first session, the rAAV2/1, 2/8 and 2/9 CMV

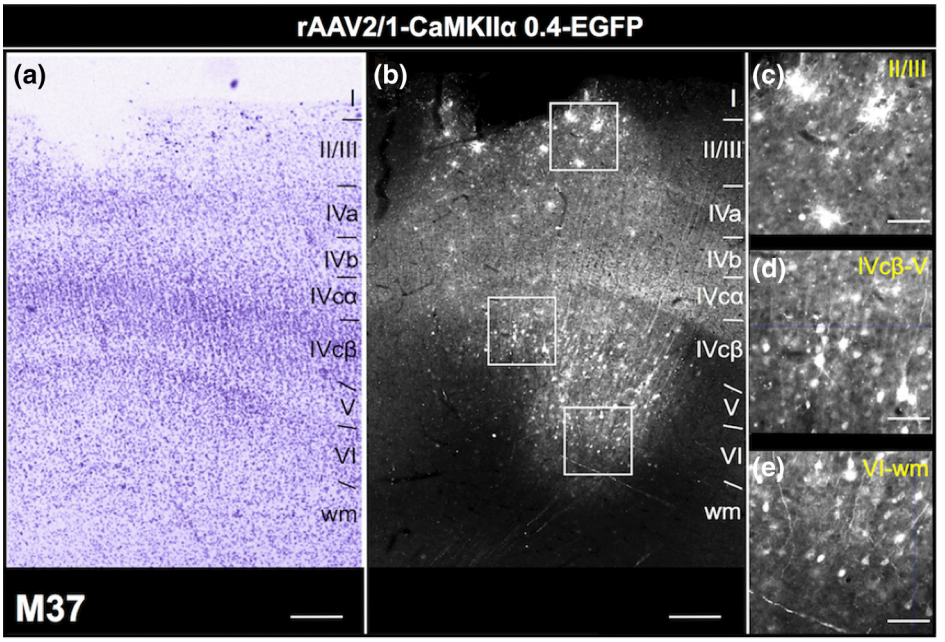

Fig. 2 Transduction patterns in V1 after rAAV2/1-CaMKIIα0.4 injection. (a) Nissl stained section used to establish the borders of the cortical layers. (b) FP+ cells on an adjacent section after injection of the rAAV2/1-CaMKIIα0.4 vector in M37. (c)–(e) Enlarged views of the sectors indicated in b (c: top, d: middle, and e: bottom frame). Scale bar in panels a and b = 200 μm. Scale bar in panels c to e = 50 μm.

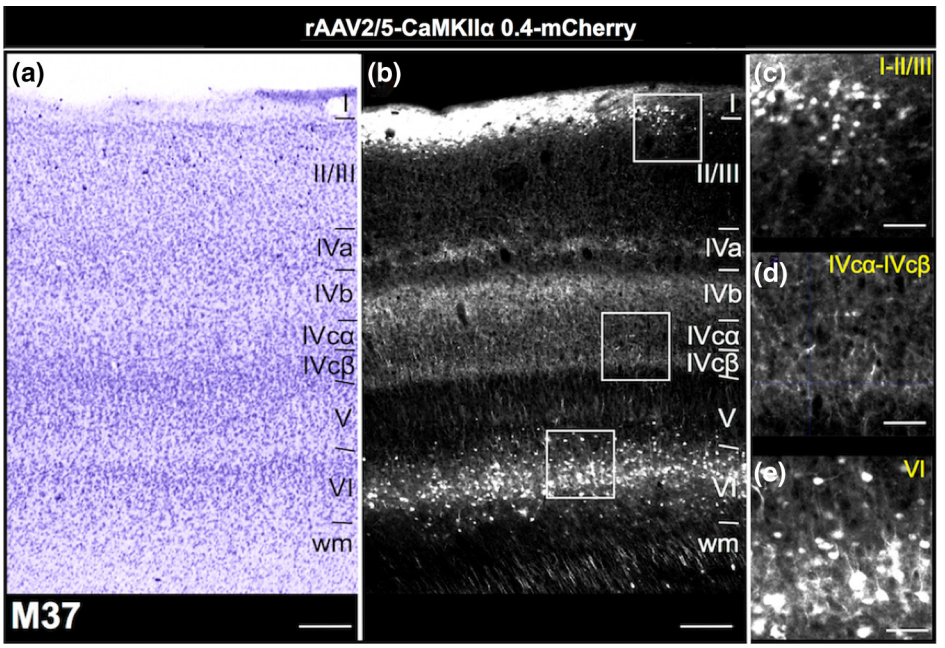

Fig. 3 Transduction patterns in V1 for rAAV2/5-CaMKIIα0.4. (a) and (b) Adjacent sections after injection of the rAAV2/5-CaMKIIα0.4 construct in V1 of M37. The left panel indicates the laminar pattern in V1. (b) FP+ expression profile across all layers. Expression of mCherry is detected mostly in the superficial and deeper layers (panels c and e). Weak FP+ expression was found in layer III and IV (panel d). Scale bar in panels a and b = 200 μm. Scale bar in panels c to e = 50 μm.

vectors and a rAAV2/7-CaMKIIα0.4 vector were injected into dorsolateral prefrontal cortex to confirm results obtained in the first monkey. In a second session, performed 6 weeks later, different serotypes (rAAV2/1, 2/5, 2/7, 2/8 and 2/9) under control of the same promoter (CaMKIIα0.4) were injected into left area V1 to compare transduction efficiencies of these serotypes with the results obtained after injections in rodent V1. In the final series of injections (3 weeks later), vectors with the same serotype (rAAV2/7), but with different promoters (CMV, enhSyn1, CaMKIIα0.4 and CaMKIIα1.3), were injected to reveal the effect of the promoter on the transgene expression. Identical injections in V1 and prefrontal cortex (area 46) were designed to compare transduction patterns across two entirely different neocortical areas.

Following a description of the FP expression at the injection sites, we will give an overview of retro-and anterograde expression patterns in the dorsal lateral geniculate nucleus (dLGN). Finally we will provide a semi-quantitative overview of the cortical FP expression patterns in a final summary figure.

3.1 *Recombinant Adeno-Associated Viral Vector Serotype-Dependent Laminar Transduction Patterns*

Figures 2 through 6 illustrate differences in transduction efficiencies and laminar FP expression patterns in striate cortex following injection of different rAAV serotypes (2/1; 2/5; 2/7; 2/8; and 2/9) under control of the CaMKIIα0.4 promoter. Vectors used for Figs. 2, 3, 5, and 6 were injected in M37, while transduction of rAAV2/7-CaMKIIα0.4 was also tested in a second monkey (M37 and M10; Fig. 4).

The rAAV2/1-CaMKIIα0.4 vector resulted in a relatively focal expression pattern covering approximately 1.2×1.0 mm^2 of cortex along the A-P and L-M axes. FP+ cells were observed in almost every layer of V1 near the injection site (Fig. 2). Transduction and EGFP expression after rAAV2/1-CaMK0.4 injection was stronger for infragranular and superficial cortical layers than in granular layers (Fig. 2). In particular, layers IVcα and IVcβ showed the weakest reporter activity in neurons. In addition to expression in neurons, positive glial cells were observed in the superficial layers [Fig. 2(c)].

Injection of rAAV2/5-CaMKIIα0.4 also yielded FP+ cells near the injection site, although a clearly less homogeneous expression pattern was observed across layers than with the rAAV2/1 vector [Figs. 2(b) and 3(b)]. Compared to rAAV2/1, neurons transduced by the rAAV2/5-CaMKIIα0.4 vector were found at substantially greater distances from the injection site along the A-P and L-M axes ($\sim 7.8 \times 5.0$ mm). The greater spread was observed mainly in the deepest layers. Transduction efficiency was especially high in layers I (fibers), VI [fibers and cells; Fig. 3(e)] and at the top of layers II/III [mostly cells; Fig. 3(c)] and relatively low in the lower part of layers II/II, layers IVcα and IVcβ and the upper part of layer V. EGFP expression was also less pronounced in layers IVa and IVb (Fig. 3).

Injection of V1 with the rAAV2/7-CaMKIIα0.4 construct yielded FP+ cells mainly in the superficial and deeper layers in both monkeys (Fig. 4). The largest fraction of transduced cells was observed in layers II/III (Fig. 4, panels c and h), followed by layer V and layer VI (Fig. 4, panels e and j). Although neuropil was FP+ in layers IVb, IVc, and IVc, these layers contained relatively few FP+ cells. Hence, this vector was less than optimal for NeuN transduction in the granular layers. The rAAV2/7-CaMKIIα0.4 vector transduced cells (mostly neurons) at greater distances from the injection site compared to rAAV2/1, but the spread parallel to the cortical surface was more restricted compared to the rAAV2/5 vector [layer VI: $(2.9 \pm 1.9) \times (2.8 \pm 0.4)$ mm; (mean $\pm$ SD) across subjects].

Injection of rAAV2/8-CaMKIIα0.4 resulted in FP+ cells through all cortical layers, with the highest fraction in the deeper layers (Fig. 5). The spread of FP-labeled cells was rather limited along the A-P and L-M axes with a slightly wider spread in the deepest layers (1.8×2.0 mm). In addition, many FP-positive glial cells were detected, most notably in the granular layers, making this serotype less specific for NeuN transduction [Fig. 5(c)].

Injection of serotype rAAV2/9 with a reporter under control of the CaMKIIα0.4 promoter transduced relatively few cells in the supragranular and granular layers in contrast to infragranular layer VI (Fig. 6). The fraction of FP+ neurons was similar to the total number of transduced cells making it better for NeuN expression in comparison to rAAV2/8 but less optimal than rAAV2/7. The spreading of FP-expression induced by this vector is again rather limited (layer VI: 1.2×2.0 mm^2).

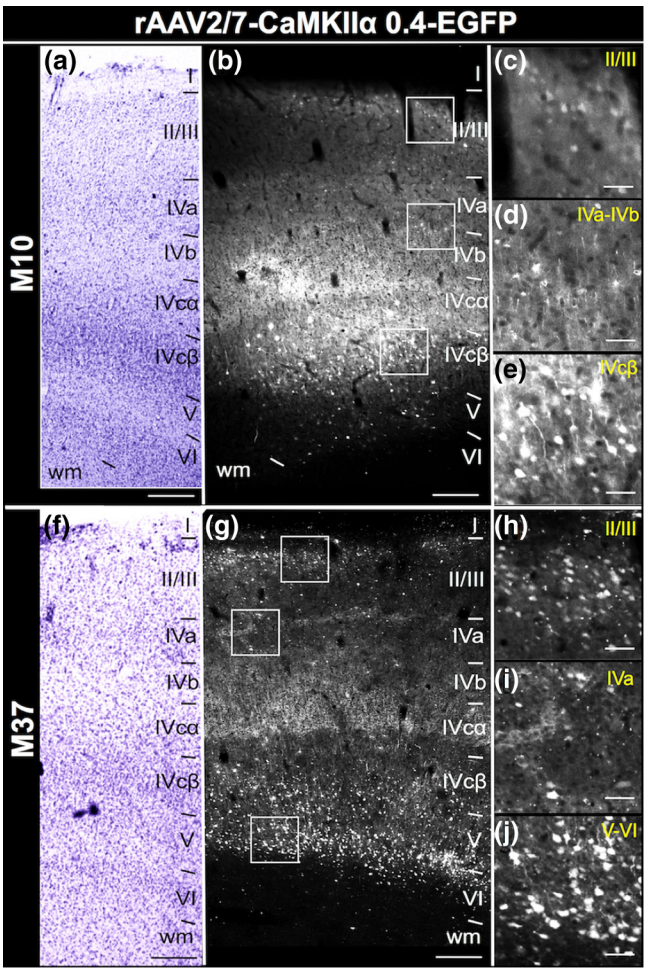

Fig. 4 Transduction patterns in V1 for rAAV2/7-CaMKIIα0.4. Transduction pattern after injection of the rAAV-CaMKIIα0.4 construct in V1 of M10 (top) and M37 (bottom). (a) and (f) show cresyl violet stained sections, middle (b and g) and right panels (c, d, e, g, h, I, j) show the EGFP expression in adjacent sections at low magnification and high magnification, respectively. Scale bars in left and middle panels = 200 μm. Scale bars for right column = 50 μm.

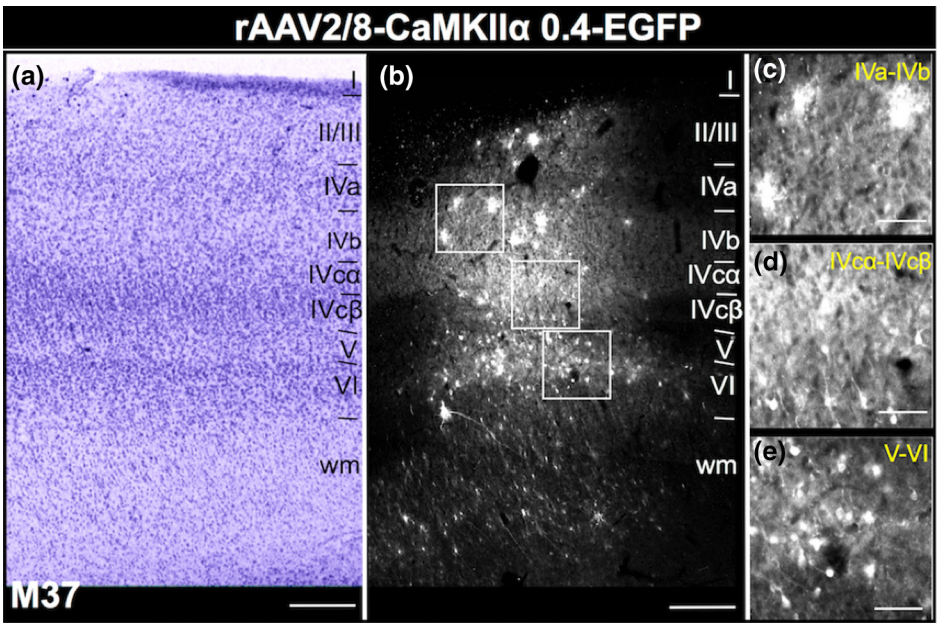

Fig. 5 Transduction patterns in V1 for rAAV2/8-CaMKIIα0.4. (a) Nissl-stained section of V1 from M37. (b) FP+ cells in an adjacent section after injection of the rAAV2/8-CaMKIIα0.4 vector in V1. Right panels (c, d, e), enlargements showing FP+ cells from the insets shown in b. Scale bars in left and middle panels = 200 μm. Scale bars for right column = 50 μm.

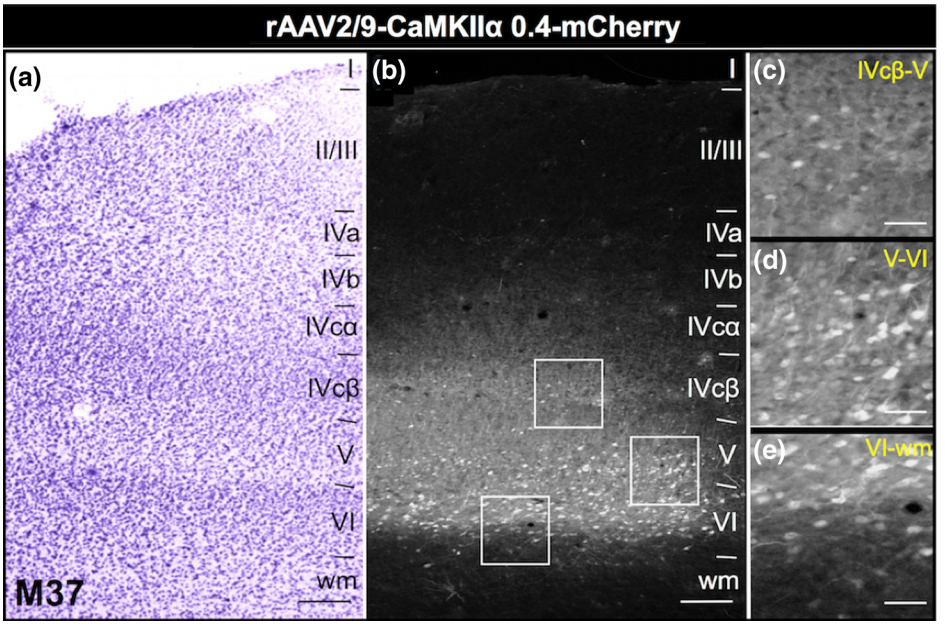

Fig. 6 Transduction patterns in V1 for rAAV2/9-CaMKIIα0.4. (a) Cresyl violet staining of V1 from M37. (b) EGFP+ cells from an adjacent section. (c)–(e) shows higher magnifications of the insets in panel (b). Scale bars in left and middle panels = 200 μm. Scale bars for right column = 50 μm.

Thus, when the CaMKIIα0.4 promoter is injected into monkey striate cortex, the number of cells that express the transgene in V1, the spread from the injection site, and the expression in the various cortical layers depend on the serotype.

3.2 *Promoter-Dependent Transgene Expression after rAAV2/7 Transduction*

We next compared transgene expression driven by different promoters while using the same rAAV serotype. We chose the rAAV2/7 serotype because the previous test yielded a high ratio of transduced neurons in both supra- and infragranular layers and also because results of a previous mouse study using exactly the same constructs as the present study showed high transduction efficiency in area V1.[23] We injected a series of rAAV2/7 vector constructs containing the CMV, enhSyn1, CaMKIIα0.4, or CaMKIIα1.3 promoters. These rAAV2/7 constructs were injected into V1 of both animals, with the exception of enhSyn1 (M37 only).

The transduction pattern induced by the rAAV2/7-CaMKIIα0.4 vector has already been described above (Fig. 4). Surprisingly, when the longer version of the CaMKIIα promoter was used (rAAV2/7-CaMKIIα1.3), a remarkably different laminar expression pattern emerged (Fig. 7). In addition to transducing cells in layers II/III, V, and VI, as with the rAAV2/7-CaMKIIα0.4 vector, the rAAV2/7-CaMKIIα1.3 vector also strongly transduced cells in layers IVa and IVb [Figs. 7(d) and 7(i)]. Furthermore, in contrast to the short CaMKIIα0.4 promoter, hardly any FP+ neurons were found in layer IVcβ (compare Figs. 4 and 7). Overall, the long CaMKIIα promoter resulted in a more efficient transgene expression and labeled cells at greater distances from the injection site than the short promoter (A-P × L-M; layer VI: $[7.7 \pm 3.2] \times [4.8 \pm 2.5]$ versus $[2.9 \pm 1.9] \times [2.8 \pm 0.4]$ mm; mean ± SD of both monkeys for the long versus short CaMKIIα promoter).

The rAAV2/7-CMV vector used in the present study displayed reasonable reporter levels throughout primary visual cortex (Fig. 8). Moreover, EGFP expression was lowest in layers II/III [Fig. 8(c)] and maximal in the deeper layers [Fig. 8(e)]. The majority of the EGFP+ cells after rAAV2/7-CMV injection, however, were non-neural [Fig. 8(b) inset]. In M10, only a few PF+ cells and fibers were detected and no transduced neurons could be found; hence, this monkey was not used for illustrating this vector.

In the second monkey, we injected a vector for which the enhancer region of a CMV promoter[53] was fused with the human Synapsin promoter[35,54,55] (i.e., enhSyn1). This promoter in a rAAV2/7 vector yielded a relatively homogeneous transgene expression across all cortical layers (Fig. 9) and resulted in FP+ cells at larger distances from the injection site compared to the rAAV2/7-CMV vector. Furthermore, a semiquantitative analysis revealed that the fraction of FP+, non-neural cells was very low (<2%) compared to the CMV promoter (>90%), which renders the former vector more suited for transduction in V1.

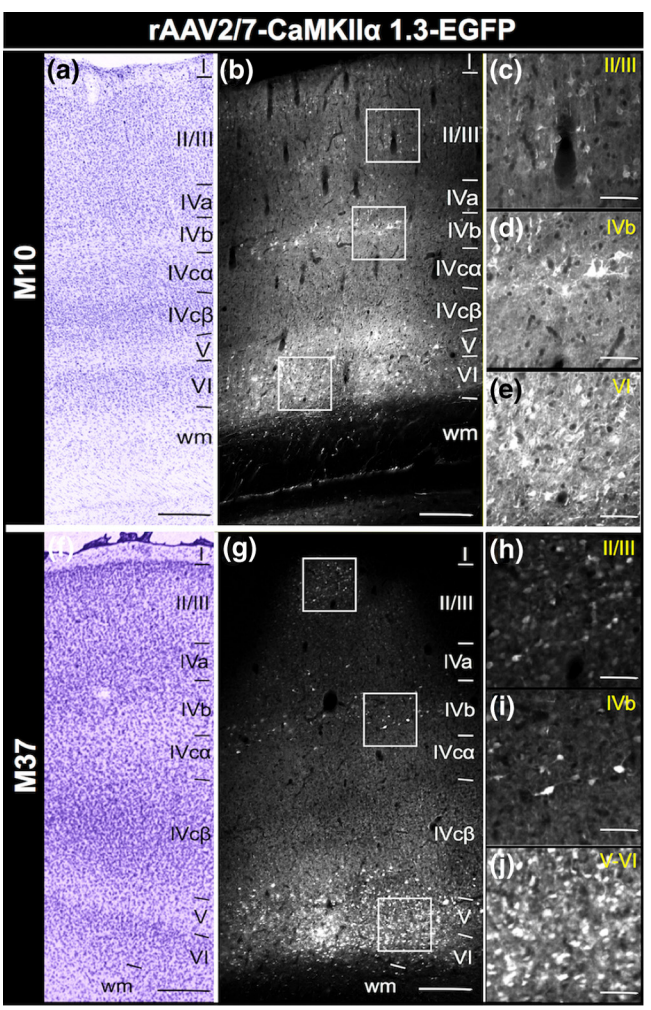

Fig. 7 Transduction patterns in V1 for rAAV2/7-CaMKIIα1.3. (a) and (f) Nissl-stained sections of V1 are shown for M10 (top) and M37 (bottom). (b) and (g) Transduction pattern of the rAAV2/7-CaMKIIα1.3 vector on adjacent sections. (c), (d), (e), (h), (i), (j) Higher magnified sections as indicated in the insets are shown on the right. Scale bars in left and middle panels = 200 μm. Scale bars for right column = 50 μm.

3.3 *Cell Specificity of a Long and Short Version of the CaMKIIα Promoter*

Viral vectors are the most efficient means with which to transfer genetic material into the central nervous system. Specific expression of a reporter or a therapeutic protein is conditional on the combination of serotype and promoter.[17,56] Here, we tested whether the CaMKIIα promoter is specific for excitatory cells, as is generally assumed.[42,43] Therefore, we performed double stainings between FP+ cells and the inhibitory cell marker (PV), which is expressed by 75% of the inhibitory cells in primate striate cortex.[57] We calculated the number of FP+ neurons that were also PV+ after injection of two rAAV2/7 vectors driven by either a short or a long CaMKIIα promoter.

No overlap was found between FP+ and PV+ cells after injecting the rAAV2/7-CaMKIIα0.4 vector [Figs. 10(a) and 10(c)]. Surprisingly, however, injection of the rAAV2/7-CaMKIIα1.3 vector yielded double-stained cells in both monkeys, indicating that at least a fraction of the cells transduced with this CaMKIIα promoter is inhibitory in nature [Figs. 10(b) and 10(d)]. We next calculated the fraction of neurons that are both PV+ and FP+. As shown in Fig. 10(e) (pooled data, M10 and M37), the short promoter revealed no overlap between FP+ and PV+ neurons. Injections with the CaMKIIα1.3 viral vector construct resulted in $3.2 \pm 0.1\%$ double-stained FP+ PV+ neurons across all the layers in V1. When considering the fraction of PV+ neurons that are also FP+ [Fig. 10(e), solid purple curve] for each layer, we found that up to 29% of the FP+ cells in layer IVcα are PV+, 17% in IVcβ, and 13% in layer V. For the other layers, the degree of overlap was below 2%. Since the highest proportion of PV+ cells is found in layer IVc,[57] this might explain why we found the highest percentage of FP+PV+ neurons in this layer. Hence, the CaMKIIα0.4 promoter is more specific for excitatory cells than the longer CaMKIIα1.3 promoter.

Although genomic titers were comparable between the two vectors, differences between CaMKIIα0.4 and CaMKIIα1.3 in their specificities for excitatory cells could be due to different functional titers. For this reason, the functional titers of rAAV2/7-CaMKIIα0.4 and rAAV2/7-CaMKIIα1.3 were determined by dilution assays (Fig. 11) (see also Ref. 23). The dilution of the viral vector solution influenced the measured titers ($p < 0.001$) but not the genomic titer of the vector construct ($p = 0.152$). Thus, because the same dilutions were injected for these vectors, differences in functional titers cannot explain the differential specificity for excitatory neurons in these two promoter sequences.

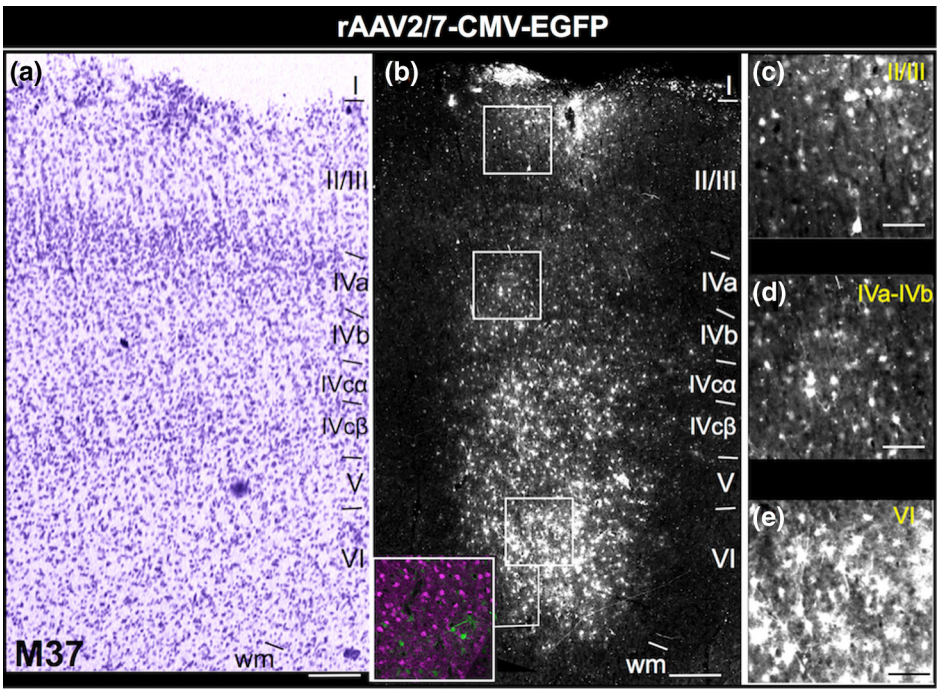

Fig. 8 Transduction patterns in V1 for rAAV2/7-CMV. (a) Cresyl violet staining of V1 in M37. (b) Transduction pattern in an adjacent section after injection of V1 with the rAAV2/7-CMV vector. The inset in layer VI (panel b) shows limited overlap between FP+ labeled cells (EGFP staining; green) and neurons (NeuN-staining; magenta). (c)–(e) Higher magnification insets showing that most FP+ cells were non-neural (i.e., no overlap between NeuN and EGFP staining). Scale bars in left and middle panels = 200 μm. Scale bars for right column = 50 μm.

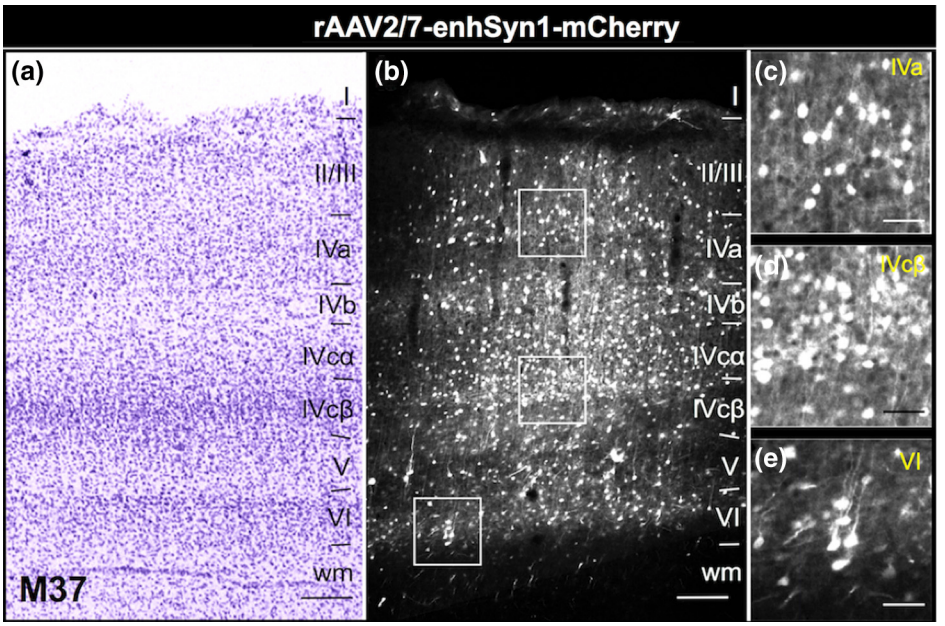

Fig. 9 Transgene expression patterns in V1 for rAAV2/7-enhSyn1-mCherry. (a) Nissl-stained section of V1 of M37. (b) Transduction pattern of the rAAV2/7-enhSyn1 vector for an adjacent section. (c)–(e) High magnification images of the insets shown in b. Scale bars in left and middle panels = 200 μm. Scale bars for right column = 50 μm.

3.4 *Projections to the Dorsal Lateral Geniculate Nucleus*

One generally assumes that rAAV viral vectors do not transfer trans-synaptically.[58] Thus, FP+ cell bodies found at greater distances from the injection site are labeled retrogradely via transduced fibers entering the injection site. The retrograde capacity of rAAV2 vectors was previously shown by Towne et al.[59] and Zhang et al.[60] Since the dLGN is bidirectionally connected with area V1, we hypothesized that this thalamic nucleus

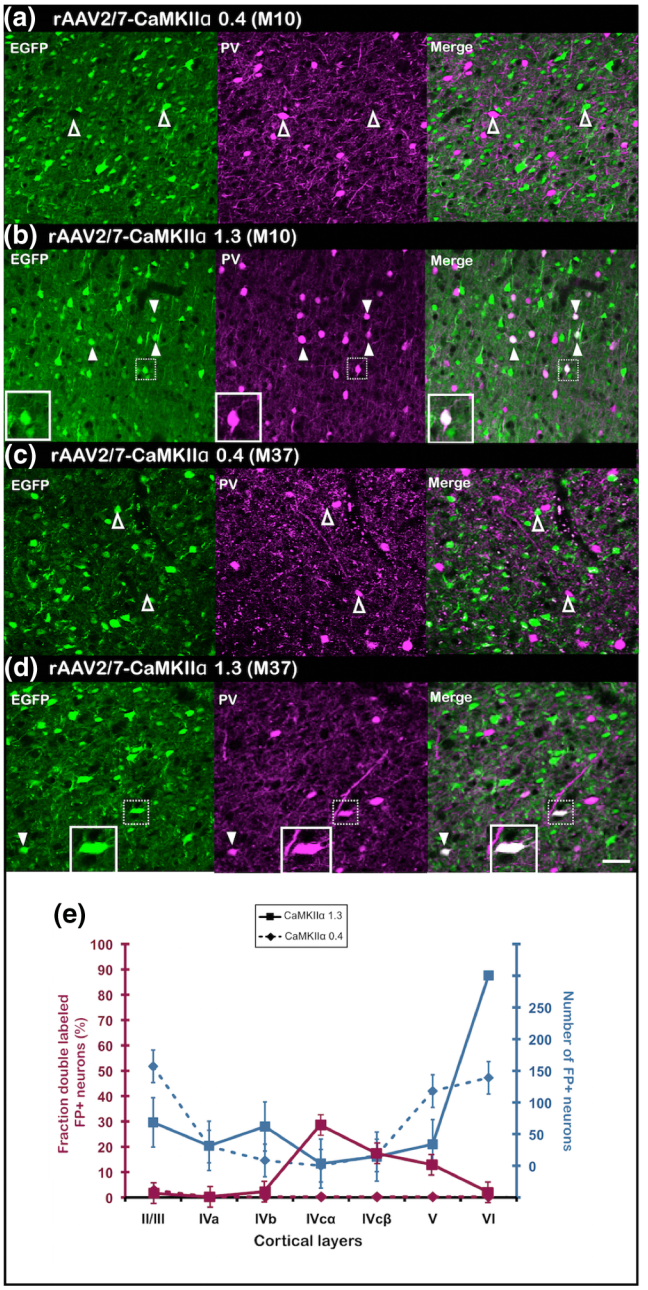

Fig. 10 Cell specificities of rAAV2/7-based vectors with long and short CaMKIIα promoters. (a) and (b) Transduction patterns in V1 of M10 using the rAAV2/7-CaMKIIα0.4 and rAAV2/7-CaMKIIα1.3 vectors, respectively. (c) and (d) Transduction patterns using the same vectors are shown for M37. The left column shows the EGFP signal (green), the middle column shows the results of PV-staining in magenta. The right column shows the merged EGFP- and PV stainings (white are double-stained neurons). The open white arrowheads indicate examples of nonoverlapping neurons and the filled white arrowheads indicate examples of EGFP+ −PV+ neurons. The inset in panels b and d illustrates double-stained neurons at higher magnification. (e) The plot illustrating the fraction of overlapping PV+ and EGFP+ neurons (%) for each cortical layer at the injection site for the CaMKIIα0.4 (dashed purple line with diamonds), and CaMKIIα1.3 promoters (solid purple line with squares). The blue plot represents the number of FP+ neurons for both the short (dashed line with diamonds) and long CaMKIIα (solid line with squares) promoters to illustrate the low proportion of FP+ neurons in the layers containing a high fraction of FP+ and PV+ overlapping cells. Data from both monkeys (M10 and M37) are pooled. Error bars represent SEM across monkeys ($n = 2$). Scale bar = 20 μm.

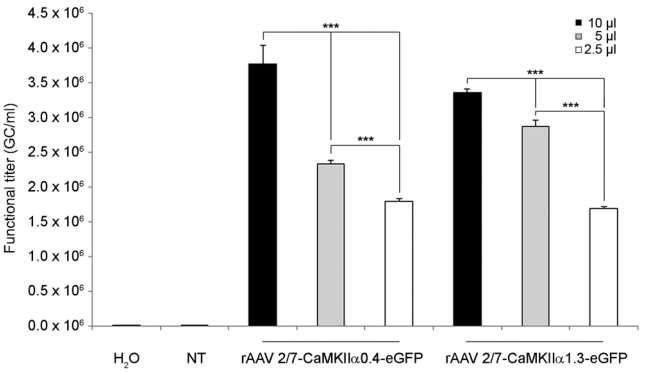

Fig. 11 Functional titers of rAAV2/7–CMV and rAAV2/7-CaMKIIα0.4. The functional titer in GC/ml was determined for three different dilutions of vector added to HEK-293T cells (black bars = 10 μl, gray bars = 5 μl, and white bars = 2.5 μl volumes). Only the volume has an effect on the functional titer. No differences exist between the serotypes. Water and nontransduced cells were added to the DNA measurements as controls. ***$p < 0.001$.

could contain both anterogradely labeled FP+ axon terminals and retrogradely labeled FP+ cell bodies.

Figure 12 shows coronal sections of the left and right dLGN with an illustration of the retinotopic maps in panels a and b.[61] Panels c and d show, respectively, EGFP+ fibers [Figs. 12(c) and 12(d)] and cells [Fig. 12(d)] in the dLGN of M10. The FP+ positive fibers in the left dLGN [Fig. 12(c); M10] must originate from the rAAV2/7-CaMKIIα0.4 vector construct, since the injection site of this vector corresponded retinotopically with the location of the FP+ signal in the dLGN and this vector construct transduced the highest proportions of neurons in left V1. In the right dLGN, we also observed FP-labeled cell bodies, which are transduced by the rAAV2/7-CaMKIIα1.3 vector [Fig. 12(d)]. Figures 12(e)–12(h) show FP+ fibers in the left and right dLGN of M37. Panels e and f reveal EGFP+ fibers, while the fibers in panels g and h are mCherry+. Since more than one of the vectors injected in each hemisphere contained the EGFP or mCherry fluorescent tag, we relied on the detailed retinotopic location of the respective injection sites in V1 and transduced fibers in the LGN to define which vector had transduced these fibers. Based on the corresponding retinotopic locations (eccentricity and polar angle) of the injection sites, we inferred that the band of fibers in panel e was transduced by the rAAV2/8-CaMKIIα0.4 vector and those in panel g by the rAAV2/5-CaMKIIα0.4 vector (approximate eccentricity and polar angle values of, respectively, 6 to 8 deg and +15 deg and 2 to 3 deg and +30 deg). The latter vector also resulted in a relatively widespread cortical transduction pattern in layer VI of V1, which can explain the broad signal corresponding to fibers projecting to the dLGN. For the right dLGN of M37, we again used retinotopic criteria to determine that the observed EGFP+ fibers are transduced by the rAAV2/7-CaMKIIα0.4 vector [eccentricity and polar angle of 4 to 6 deg and +15 deg; Fig. 12(f)], and the mCherry+ fibers in the left dLGN by the rAAV2/7-enhSyn1 vector [eccentricity and polar angle of 4 to 6 deg and −15 deg; Fig. 12(h)]. No signal corresponding to the injection of rAAV2/1-CaMKIIα0.4, rAAV2/9-CaMKIIα0.4 and of the CMV driven vectors was found in the LGN, indicating poor anterograde and retrograde transport to this thalamic nucleus after injection of these viral vectors in V1.

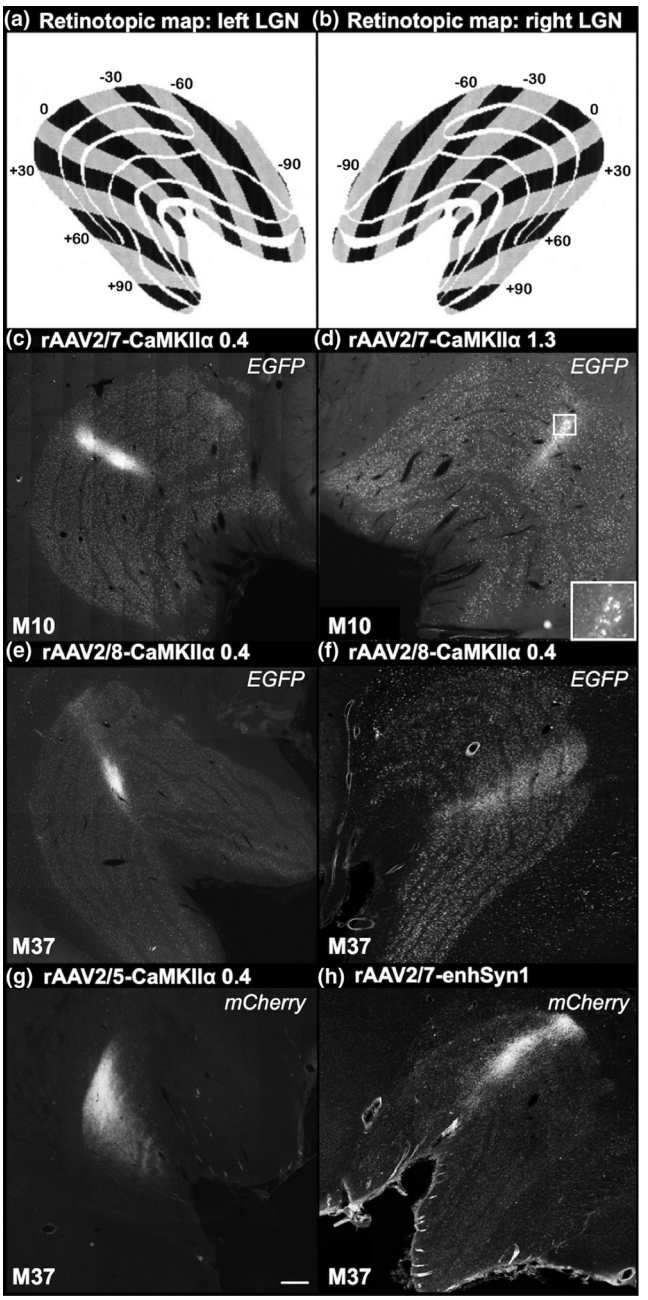

Fig. 12 Retinotopic-specific antero-and retrograde transduction in dLGN after injection of rAAV vectors in V1. (a) and (b) Retinotopic map of a coronal section of the left and right LGN as determined by Malpeli and Baker[61] (reprinted with permission). (c) and (d) Retinotopic-specific, anterogradely labeled fibers and retrogradely labeled cells in the LGN after injection of rAAV2/7-CaMKIIα0.4 and rAAV2/7-CaMKIIα1.3 in V1 of M10, respectively. In M37, (e) and (f) EGFP-positive fibers and (g) and (h) mCherry-positive fibers were found. The FP+ fibers in panels (e) and (g) are induced by V1 injections with the rAAV2/8-CaMKIIα0.4 and rAAV2/5-CaMKIIα0.4 vectors, respectively. In panels (f) and (h) (right LGN), the EGFP+ fibers are induced by rAAV2/7-CaMKIIα0.4 and rAAV2/7-enhSyn1 injections in V1, respectively. Scale bar = 500 μm.

Thus, injection of rAAV2/7-CaMKIIα0.4, rAAV2/7-CaMKIIα1.3, rAAV2/7-enhSyn1, rAAV2/5-CaMKIIα0.4, and rAAV2/8-CaMKIIα0.4 in V1 resulted in anterogradely labeled FP+ axon terminals in the LGN, whereas retrogradely labeled FP+ cell bodies were found only after rAAV2/7-CaMKIIα1.3 vector injections.

3.5 *Comparison of rAAV2/7-Mediated Transduction Patterns in V1 and Dorsolateral Prefrontal Cortex*

First, to determine whether the transduction efficiencies and expression patterns described in the present study are specific for V1 or are similar in different cortical areas, one vector (rAAV2/7-CaMKIIα0.4) was injected in area V1 and in the dorsolateral prefrontal cortex (area 46) of one monkey (M37). Transduction was more homogeneous across all layers of area 46 compared to V1 (Fig. 13), but the area of lateromedial spread in layer VI was half of that in area 46 (2.4 mm versus 5.0 mm). The anteroposterior spread, however, was equal in the two areas (3.0 mm).

3.6 *Comparison of Cytomegalovirus-Mediated Transduction Patterns in V1 and Dorsolateral Prefrontal Cortex*

Finally, to confirm that the absence of FP+ neurons after injection of the CMV-promoter-driven constructs is not restricted to V1, the same vectors were also injected into area 46. All injected CMV- constructs (rAAV2/1-CMV, rAAV2/8-CMV and rAAV2/9-CMV) failed to show transgene expression in prefrontal cortical neurons in macaque neocortex.

4 Discussion

We injected a series of rAAV serotypes (rAAV2/1; 2/5; 2/7; 2/8; 2/9) controlled by multiple promoters (CaMKIIα0.4, CaMKIIα1.3, CMV, and enhSyn1) into primary visual and dorsolateral prefrontal cortex of rhesus monkey and studied the transduction efficiency, spread and laminar expression based on cellular EGFP or mCherry fluorescent reporter gene expression.

4.1 *Transduction Efficiencies are Serotype Dependent*

Primate cortical neurons were successfully transduced with rAAV2/1, rAAV2/5, rAAV2/7, rAAV2/8, and rAAV2/9. Earlier reports by Markakis[39] and Dodiya[41] showed variations in the number of macaque neurons transduced depending on the serotype used. In these previous reports, rAAV2/1 and rAAV2/5 proved the most efficient vectors. They transduced a large number of cells in the basal ganglia, striatum, and substantia nigra (SN) of the primate brain. Other studies with injections in the SN of rats reported higher transduced brain volumes using rAAV2/7, rAAV2/9, and rAAV2/1 than with rAAV2/8 and rAAV2/5, indicating species-dependent transduction efficiencies of the viral vectors.[30,33,62] In our study, the rAAV2/1-CaMKIIα0.4 showed efficient transduction at the injection site but the transgene expression pattern was limited to about 1.2×1.0 mm^2. This corroborates a recent report by Jazayeri et al.[54] in which the rAAV2/1 vector, including the hSyn promoter, was injected into this same cortical area. These authors reported a small band of ChR2-positive cells at the injection site, with only a few transduced neurons 1 mm away. Furthermore, despite uniform injection throughout the cortical depth, they also found layer-specific expression of the gene-of-interest, possibly due to the characteristic tropism of the rAAV2/1 vector.[54]

Vector rAAV2/5 has been reported to disperse further from the injection site in both mice and primates.[23,32,35,63] Also in the present study, rAAV2/5-CaMKIIα0.4 injections resulted in the

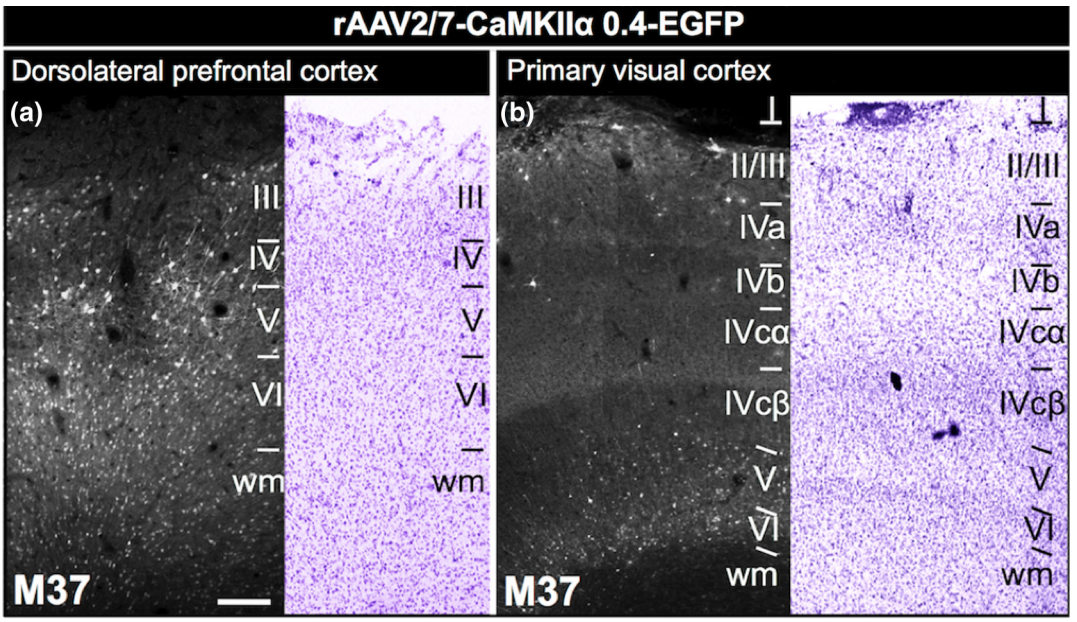

Fig. 13 Comparison of transduction patterns in V1 and prefrontal cortex. (a) and (b) Transduction pattern of rAAV2/7-CaMKIIα0.4 in the dorsolateral prefrontal cortex and in the primary visual cortex. The left images show the FP+ cells. The figures on the right are the corresponding photographs of Nissl staining. Scale bar is 200 μm.

most widespread (7.8×5.0 mm^2) transduction across layers II/III, V, and VI. Other serotypes, such as rAAV2/7, showed a spread of $(2.9 \pm 1.9) \times (2.8 \pm 0.4)$ mm (i.e., mean of both monkeys $\pm$ SD), while rAAV2/8 and rAAV2/9 showed smaller spreads [(1.8×2.0) and (1.2×2.0) mm, respectively]. We summarized the results of our semiquantitative comparisons in Fig. 14 and ranked the AAV serotypes containing the CaMKIIα0.4-promoter by transduction efficiency based on the cortical spread: rAAV2/5>>rAAV2/7>rAAV2/8>rAAV2/9>>rAAV2/1. This ranking differs only for rAAV2/8 and rAAV2/9 from that reported for mouse visual cortex using exactly the same vector batches (rAAV2/5 >> 2/7 $\geq$ 2/9 $\geq$ 2/8 >> 2/1),[23] but more substantially with regard to primate SN, striatum, and basal ganglia (rAAV2/5 $\geq$ rAAV2/1 > rAAV2/8[39,41]).

Additionally, for the percentages of transduced neurons at injection sites, we could rank the rAAV serotypes as follows: rAAV2/1>rAAV2/5>rAAV2/7=rAAV2/9>rAAV2/8. When aiming for an rAAV serotype with a high percentage of transduced cells at the injection site and a widely spread transduction, the ranking is as follows: rAAV2/5 > rAAV2/7 > rAAV2/1 > rAAV2/8 = rAAV2/9 (see Fig. 14).

4.2 *Promoter-Dependent Transgene Expression Levels*

The serotype of the vector determines which cells can be transduced by the viral particles. Furthermore, the promoter should also be active in expressing the reporter protein in these cells. Thus, the combination of serotype and promoter determines the transduction pattern. Despite the widespread use of the CMV promoter in rodents,[32,33,64–66] we were unable to transduce neurons efficiently with rAAV carrying the CMV promoter in primate cortical neurons, in both visual and prefrontal cortices. Recently, Watakabe et al.[18] reported neural toxicity caused by the CMV promoter when survival time after injections exceeded 21 days (in our case between 29 and 93 days). In line with this study, we also found more than 90% of the transgene expression driven by rAAV2/7 CMV in glial cells instead of neurons.

In contrast to results with the CMV promoter, the human synapsin-1 promoter[11,35,55] combined with the enhancer elements of the CMV promoter (enhSyn1) yielded a homogenous expression pattern across all cortical layers. The hSyn1 promoter sequence efficiently recruits TFs in monkey neurons based on the high expression levels driven by the enhSyn1 promoter in these cells. In rodents, NeuN TFs have been shown to have a high affinity for the hSyn1 promoter.[63,64] Adding the CMV enhancer sequence (enhSyn1) additionally improves the neuron-specific transcriptional activity of the hSyn1 promoter, in line with previous reports.[67,68]

Another surprising finding was the different transduction patterns induced by two highly similar viral vector constructs consisting of different lengths (364 bp and 1291 bp) of the CaMKIIα promoter. We found that in V1, the short 0.4 kb CaMKIIα-promoter transduces neurons in all layers, with the least efficiency in layers IVb and IVcα. The long version CaMKIIα-promoter selectively transduced cells in all cortical layers, however, few neurons in layer IVcα and IVcβ. Thus, the main distinction between the transduction efficiencies of these two versions of the CaMKIIα promoters can be found in the granular layers. The laminar expression of CaMKIIα mRNA in primate V1 has been well described [69–71] but fails to explain the differences we observed between the transduction patterns of the two versions of the CaMKIIα promoters used in this study. For instance, layer IVb is almost void of CaMKIIα mRNA signal,[69,71] which fits with the low number of transduced cells in layer IVb using the CaMKIIα0.4 promoter but not with the reasonably high transduction levels using the CaMKIIα1.3 promoter. Based on the lack of expression in specific layers using the CaMKIIα1.3 promoter, we speculate that factors that can inhibit transcription, such as specific miRNAs, may bind to the extra fragments in the longer version of the

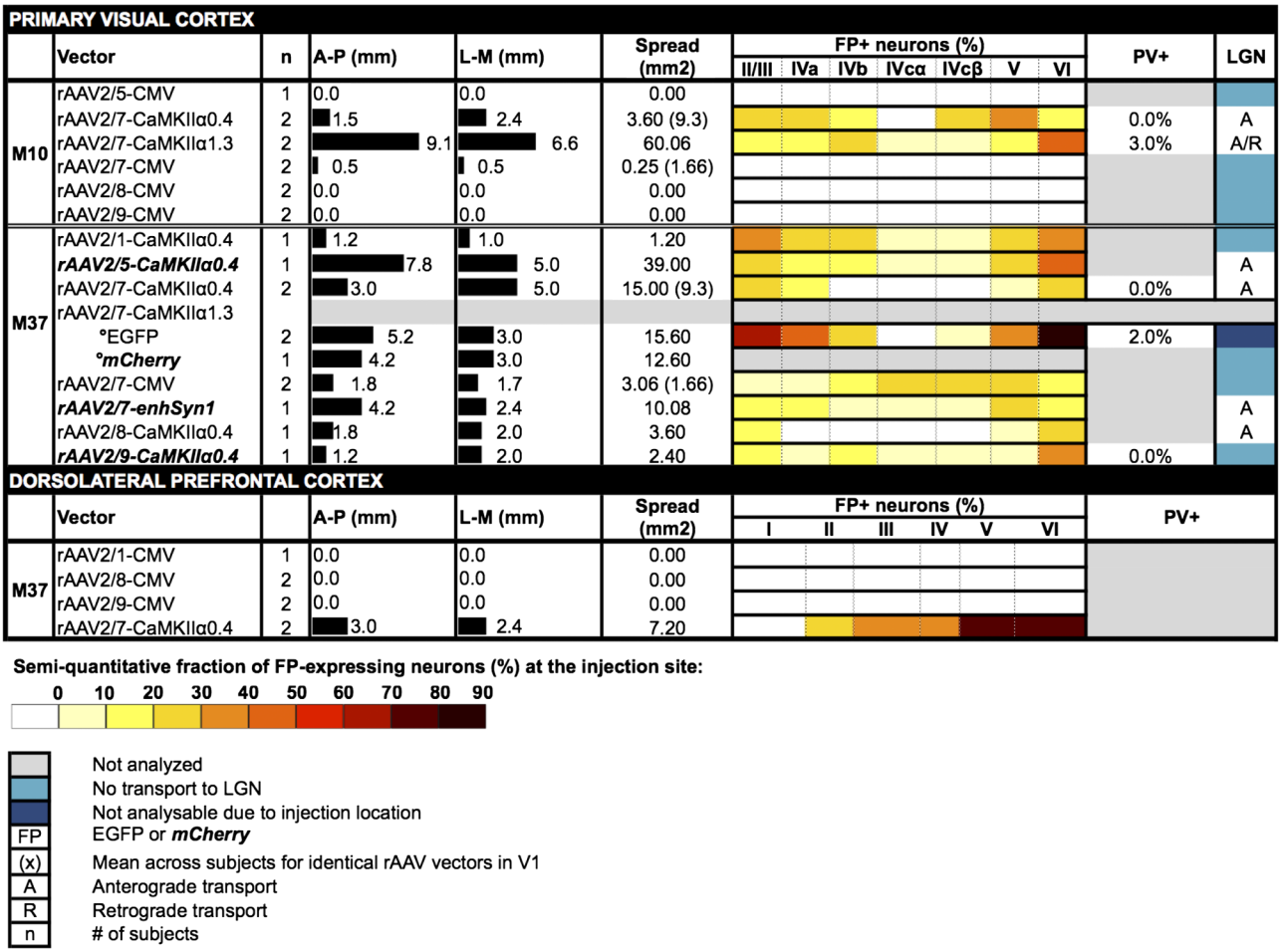

Fig. 14 Semiquantitative summary of the transduction results in M10 and M37. This figure shows a semiquantitative overview of the results (the spread along the cortical surface and fraction of FP+ neurons) for each injected vector in the primary visual cortex (M10 and M37) and dorsolateral prefrontal cortex (M37). Columns 4 and 5 illustrate the spread of FP-labeled cells (black bars) along the anterior–posterior axis (A-P) and lateral–medial axis (L-M), respectively. Column 5 represents the product of columns 3 and 4 (two-dimensional spread). Column 6 shows the percentage of EGFP+ neurons at the injection site (300 μm in L-M direction) for individual layers. Column "PV+" shows the percentage of parvalbumine-positive labeled EGFP+ neurons. The last column (LGN) shows anterograde (A)- or retrograde (R) transduction capability in the LGN as a result of vector injections in V1. Numbers between brackets correspond to the mean values across monkeys (when available).

CaMKIIα promoter. Conversely, higher expression levels induced by the CaMKIIα0.4 promoter may result from the loss of this inhibitory regulation. Irrespective of the reasons for transductional disparities between the short and long CaMKIIα promoters, the former is more specific for excitatory cells when used in combination with AAV.

Other than the specific laminar expression patterns of the two CaMKIIα-promoters, differences in cell specificity were also observed. The rAAV2/7-CaMKIIα0.4 vector resulted in transgene expression exclusively in excitatory neurons while, somewhat surprisingly, rAAV2/7-CaMKIIα1.3 also drove expression in a small proportion of V1 PV-positive cells. Despite the relatively small fraction of PV+FP+ neurons across the cortical depth as a whole, in some layers (e.g., IVcα) almost one third of the transduced neurons were inhibitory in nature. The latter results are contrary to findings in most nonhuman primate[42,43] and rodent studies,[49,51,52,72] where selective expression in excitatory cells was reported when the CaMKIIα promoter is used. A study by Nathanson et al.[46] already showed the lack of specificity of the CaMKIIα promoter when used in an AAV vector, and recent results in mice have confirmed this finding.[50] Furthermore, these authors reported that the specificity of lentiviral vectors with the CaMKIIα promoter is largely due to the tropism of the lentivirus, in which the CaMKIIα can provide additional selectivity. Also in line with our results, the fugu-derived CaMKIIα promoter in an rAAV2/1 vector drives expression in a small fraction of inhibitory neurons.[73] In that study, the percentage of excitatory positive-labeled cells was much higher, exactly as in the present study.

4.3 *Retrogradely Transduced Cells*

Previous studies showed that rAAVs can transduce cells retrogradely in nonhuman primates[39,58,74,75] and rodents.[30,32,76–79] We confirmed this observation by showing EGFP-labeled cell bodies in the dLGN at locations corresponding retinotopically to the V1 injection sites of the rAAV2/7-CaMKIIα1.3 vector. The degree of retrograde labeling was rather low. Injections

of the rAAV2/7-CaMKIIα0.4, rAAV2/5-CaMKIIα0.4, rAAV2/8-CaMKIIα0.4, and rAAV2/7-enhSyn1 vectors in V1 resulted only in anterogradely FP-labeled axons in retinotopically matching regions of the dLGN. The differences in retro-and anterograde transduction capacities in the dLGN may be related to the laminar variations in transduction observed in area V1 using the various vectors in the present study. Thalamocortical axons terminate mainly in layer IV;[80] hence, good transduction of that layer should be required for optimal retrograde labeling in the LGN. Conversely, feedback from V1 to the LGN mainly originates in layer VI; thus, efficient transduction in the deepest layer after V1 injections must be a prerequisite for good anterograde labeling in the thalamus.

4.4 *Transduction Efficiencies are Area Dependent*

We found laminar differences in the transduction patterns in two neocortical areas (V1 and prefrontal cortex) of the same monkey, even when injecting the same viral vector (Fig. 13). Hence, as expected, the transduction pattern of rAAV vectors also depends on the targeted area. This suggestion is corroborated by the apparent discrepancy between our results and those obtained in primate SN using the same serotype.[30] The lack of FP+ neurons after injecting a CMV construct, however, was observed in the two neocortical areas. This could indicate that the aforementioned neural toxicity caused by CMV-driven constructs affects all cortical regions.

4.5 *Limitations*

4.5.1 *Titer does not explain differences in neuronal transduction patterns*

In the present study, a similar volume was injected for all vector constructs. Several of the viral vector constructs, such as rAAV2/7-CaMKII0.4, rAAV2/8-CaMKII0.4 and rAAV2/9-CaMKII0.4, had almost equal genomic titers (2.6, 2.8, and 3.1 E12 gc/ml, respectively). These constructs, however, resulted in markedly different numbers of transduced cells and yielded pronounced differences in the spreads of the transduction patterns along the cortical sheet (see Fig. 14). The functional titer essay also argues against genomic titer being an explanatory factor for the observed differences in FP expression patterns (Fig. 11). In addition, similar results with identical viral vectors were found in the mouse visual cortex.[23] We, therefore, suggest that the main factors driving the variations in transduction efficiencies are the serotype, the promoter, and the injected cortical area.

4.5.2 *Sample size*

Although this study provides useful insights into the transduction capacity of viral vectors in primates, it has its limitations. Sample size was low (i.e., multiple injections were only performed in one animal) and differences in time between injection and perfusion could have produced variations in transductional profiles. Optimal timing for transduction and expression of rAAV may vary according to viral vector, injection area, and species.[81] Nevertheless, previous results in monkeys showed a stable expression of AAV2 after 30 days.[39] Although a staining for inflammatory responses was not performed in this study, obvious inflammatory tissue damage was not discernable. Correspondingly, a comparison of blood samples taken from M37 before and after injection did not reveal any immune responses.

5 Conclusion

The present study compared NeuN tropism of rAAVs in macaque cortex. Our results illustrated that different rAAV constructs (various recombinant AAV vectors in combination with different promoters) yield distinct transgene expression patterns in terms of spread, laminar distribution, cell specificity, and retrograde transduction capacities. The comparison of multiple viral vector systems within the present study and across previously published studies revealed that transduction patterns of viral vector systems depend on (1) the serotype, (2) the promoter sequence, and (3) the targeted area. Given the variability in transduction efficiency obtained using various rAAV constructs, we advise performing histological checks in each viral vector-based experiment. More provocatively, these results indicate that by selecting the appropriate combination of vector and promoter, one may target specific NeuN circuits within primate striate cortex, confined to specific layers and types of neurons.

Acknowledgments

We thank J. Aerts, I. Scheyltjens, and S. Raiguel for their technical support and valuable comments on this manuscript. We also thank C. Van Eupen and I. Puttemans for their technical assistance during the surgeries and P. Kayenbergh and G. Meulemans for technical support. Viral vector production was done at the Leuven Viral Vector Core with the help of N. J. Van der Veken, I. Thiry, S. De Swaef, W. Werckx and S. Deman. This work received support from IWT-SBO 110068 (Optobrain), FWO Vlaanderen G090714N, G088813N, G083111N10, EF/05/014, GOA/10/019, FP7-ICT-2011-C Enlightenment, Odysseus G0007.12, Hercules AKUL/09/038 and IUAP 7/11. A.G. is a postdoctoral fellow of the FWO Vlaanderen. P.V. is a doctoral fellow supported by the Agency for Innovation by Science and Technology in Flanders (IWT). ME.L. is a postdoctoral fellow of FRQS.

References

1. W. T. Hermens and J. Verhaagen, "Viral vectors, tools for gene transfer in the nervous system," *Prog. Neurobiol.* **55**(4), 399–432 (1998).
2. N. Deglon and P. Hantraye, "Viral vectors as tools to model and treat neurodegenerative disorders," *J. Gene Med.* **7**(5), 530–539 (2005).
3. R. J. Mandel et al., "Recombinant adeno-associated viral vectors as therapeutic agents to treat neurological disorders," *Mol. Ther.* **13**(3), 463–483 (2006).
4. P. Osten, V. Grinevich, and A. Cetin, "Viral vectors: a wide range of choices and high levels of service," *Handb. Exp. Pharmacol.* **178**, 177–202 (2007).
5. S. Palfi et al., "Long-term safety and tolerability of ProSavin, a lentiviral vector-based gene therapy for Parkinson's disease: a dose escalation, open-label, phase 1/2 trial," *Lancet* **383**(9923), 1138–1146 (2014).
6. T. B. Lentz, S. J. Gray, and R. J. Samulski, "Viral vectors for gene delivery to the central nervous system," *Neurobiol. Dis.* **48**(2), 179–188 (2012).
7. E. S. Boyden, "A history of optogenetics: the development of tools for controlling brain circuits with light," *F1000 Biol. Rep.* **3**, 11 (2011).
8. J. Butler, "Optogenetics: shining a light on the brain," *Biosci. Horiz.* **5** (2012).
9. K. Deisseroth, "Controlling the brain with light," *Sci. Am.* **303**(5), 48–55 (2010).
10. A. Gerits and W. Vanduffel, "Optogenetics in primates: a shining future?," *Trends Genet.* **29**(7), 403–411 (2013).
11. O. Yizhar et al., "Optogenetics in neural systems," *Neuron* **71**(1), 9–34 (2011).

12. S. Dong, S. C. Rogan, and B. L. Roth, "Directed molecular evolution of DREADDs: a generic approach to creating next-generation RASSLs," *Nat. Protoc.* **5**(3), 561–573 (2010).
13. S. M. Ferguson and J. F. Neumaier, "Grateful DREADDs: engineered receptors reveal how neural circuits regulate behavior," *Neuropsychopharmacology* **37**(1), 296–307 (2012).
14. S. C. Rogan and B. L. Roth, "Remote control of neuronal signaling," *Pharmacol. Rev.* **63**(2), 291–315 (2011).
15. M. Kinoshita et al., "Genetic dissection of the circuit for hand dexterity in primates," *Nature* **487**(7406), 235–238 (2012).
16. T. Sooksawate et al., "Viral vector-mediated selective and reversible blockade of the pathway for visual orienting in mice," *Front. Neural Circuits* **7**, 162 (2013).
17. J. N. Betley and S. M. Sternson, "Adeno-associated viral vectors for mapping, monitoring, and manipulating neural circuits," *Hum. Gene Ther.* **22**(6), 669–677 (2011).
18. A. Watakabe et al., "Comparative analyses of adeno-associated viral vector serotypes 1, 2, 5, 8 and 9 in marmoset, mouse and macaque cerebral cortex," *Neurosci. Res.* **93**, 144–157 (2014).
19. J. L. Howarth, Y. B. Lee, and J. B. Uney, "Using viral vectors as gene transfer tools (cell biology and toxicology special issue: ETCS-UK 1 day meeting on genetic manipulation of cells)," *Cell Biol. Toxicol.* **26**(1), 1–20 (2010).
20. C. Lundberg et al., "Applications of lentiviral vectors for biology and gene therapy of neurological disorders," *Curr. Gene Ther.* **8**(6), 461–473 (2008).
21. B. Jarraya et al., "Dopamine gene therapy for Parkinson's disease in a nonhuman primate without associated dyskinesia," *Sci. Transl. Med.* **1**(2), 2ra4 (2009).
22. J. H. Kordower et al., "Neurodegeneration prevented by lentiviral vector delivery of GDNF in primate models of Parkinson's disease," *Science* **290**(5492), 767–773 (2000).
23. I. Scheyltjens et al., "Evaluation of the expression pattern of rAAV2/1, 2/5, 2/7, 2/8 and 2/9 serotypes with different promoters in the mouse visual cortex," *J. Comp. Neurol.* **523**, 2019–2042 (2015).
24. K. S. Bankiewicz et al., "Long-term clinical improvement in MPTP-lesioned primates after gene therapy with AAV-hAADC," *Mol. Ther.* **14**(4), 564–570 (2006).
25. M. G. Kaplitt et al., "Long-term gene expression and phenotypic correction using adeno-associated virus vectors in the mammalian brain," *Nat. Genet.* **8**(2), 148–154 (1994).
26. R. L. Klein et al., "Dose and promoter effects of adeno-associated viral vector for green fluorescent protein expression in the rat brain," *Exp. Neurol.* **176**(1), 66–74 (2002).
27. D. M. McCarty, S. M. Young, Jr., and R. J. Samulski, "Integration of adeno-associated virus (AAV) and recombinant AAV vectors," *Annu. Rev. Genet.* **38**, 819–845 (2004).
28. T. J. McCown, "Adeno-associated virus (AAV) vectors in the CNS," *Curr. Gene Ther.* **5**(3), 333–338 (2005).
29. V. W. Choi, D. M. McCarty, and R. J. Samulski, "AAV hybrid serotypes: improved vectors for gene delivery," *Curr. Gene Ther.* **5**(3), 299–310 (2005).
30. C. Burger et al., "Recombinant AAV viral vectors pseudotyped with viral capsids from serotypes 1, 2, and 5 display differential efficiency and cell tropism after delivery to different regions of the central nervous system," *Mol. Ther.* **10**(2), 302–317 (2004).
31. J. E. Rabinowitz et al., "Cross-packaging of a single adeno-associated virus (AAV) type 2 vector genome into multiple AAV serotypes enables transduction with broad specificity," *J. Virol.* **76**(2), 791–801 (2002).
32. J. M. Taymans et al., "Comparative analysis of adeno-associated viral vector serotypes 1, 2, 5, 7, and 8 in mouse brain," *Hum. Gene Ther.* **18**(3), 195–206 (2007).
33. A. Van der Perren et al., "Efficient and stable transduction of dopaminergic neurons in rat substantia nigra by rAAV 2/1, 2/2, 2/5, 2/6.2, 2/7, 2/8 and 2/9," *Gene Ther.* **18**(5), 517–527 (2011).
34. S. Ciocchi et al., "Encoding of conditioned fear in central amygdala inhibitory circuits," *Nature* **468**(7321), 277–282 (2010).
35. I. Diester et al., "An optogenetic toolbox designed for primates," *Nat. Neurosci.* **14**(3), 387–397 (2011).
36. A. V. Kravitz et al., "Regulation of parkinsonian motor behaviours by optogenetic control of basal ganglia circuitry," *Nature* **466**(7306), 622–626 (2010).
37. J. H. Lee et al., "Global and local fMRI signals driven by neurons defined optogenetically by type and wiring," *Nature* **465**(7299), 788–792 (2010).
38. I. B. Witten et al., "Recombinase-driver rat lines: tools, techniques, and optogenetic application to dopamine-mediated reinforcement," *Neuron* **72**(5), 721–733 (2011).
39. E. A. Markakis et al., "Comparative transduction efficiency of AAV vector serotypes 1-6 in the substantia nigra and striatum of the primate brain," *Mol. Ther.* **18**(3), 588–593 (2010).
40. C. E. Sanchez et al., "Recombinant adeno-associated virus type 2 pseudotypes: comparing safety, specificity, and transduction efficiency in the primate striatum. Laboratory investigation," *J. Neurosurg.* **114**(3), 672–680 (2011).
41. H. B. Dodiya et al., "Differential transduction following basal ganglia administration of distinct pseudotyped AAV capsid serotypes in non-human primates," *Mol. Ther.* **18**(3), 579–587 (2010).
42. X. Han et al., "A high-light sensitivity optical neural silencer: development and application to optogenetic control of non-human primate cortex," *Front. Syst. Neurosci.* **5**, 18 (2011).
43. X. Han et al., "Millisecond-timescale optical control of neural dynamics in the nonhuman primate brain," *Neuron* **62**(2), 191–198 (2009).
44. W. Vanduffel et al., "Visual motion processing investigated using contrast agent-enhanced fMRI in awake behaving monkeys," *Neuron* **32**(4), 565–577 (2001).
45. H. Hioki et al., "Efficient gene transduction of neurons by lentivirus with enhanced neuron-specific promoters," *Gene Ther.* **14**(11), 872–882 (2007).
46. J. L. Nathanson et al., "Preferential labeling of inhibitory and excitatory cortical neurons by endogenous tropism of adeno-associated virus and lentivirus vectors," *Neuroscience* **161**(2), 441–450 (2009).
47. R. J. Cruz-Rizzolo et al., "Cyto-, myelo- and chemoarchitecture of the prefrontal cortex of the Cebus monkey," *BMC Neurosci.* **12**(6), 1–26 (2011).
48. G. Paxinos et al., *The Rhesus Monkey Brain in Stereotaxic Coordinates*, Academic Press, San Diego (2000).
49. J. P. Johansen et al., "Optical activation of lateral amygdala pyramidal cells instructs associative fear learning," *Proc. Natl. Acad. Sci. U. S. A.* **107**(28), 12692–12697 (2010).
50. V. S. Sohal et al., "Parvalbumin neurons and gamma rhythms enhance cortical circuit performance," *Nature* **459**(7247), 698–702 (2009).
51. K. M. Tye et al., "Amygdala circuitry mediating reversible and bidirectional control of anxiety," *Nature* **471**(7338), 358–362 (2011).
52. T. Dittgen et al., "Lentivirus-based genetic manipulations of cortical neurons and their optical and electrophysiological monitoring in vivo," *Proc. Natl. Acad. Sci.* **101**(52), 18206–18211 (2004).
53. A. Ibrahimi et al., "Highly efficient multicistronic lentiviral vectors with peptide 2A sequences," *Hum. Gene Ther.* **20**(8), 845–860 (2009).
54. M. Jazayeri, Z. Lindbloom-Brown, and G. D. Horwitz, "Saccadic eye movements evoked by optogenetic activation of primate V1," *Nat. Neurosci.* **15**(10), 1368–1370 (2012).
55. L. Yin et al., "Intravitreal injection of AAV2 transduces macaque inner retina," *Invest. Ophthalmol. Vis. Sci.* **52**(5), 2775–2783 (2011).
56. Z. Shevtsova et al., "Promoters and serotypes: targeting of adeno-associated virus vectors for gene transfer in the rat central nervous system in vitro and in vivo," *Exp. Physiol.* **90**(1), 53–59 (2005).
57. J. F. Van Brederode, K. A. Mulligan, and A. E. Hendrickson, "Calcium-binding proteins as markers for subpopulations of GABAergic neurons in monkey striate cortex," *J. Comp. Neurol.* **298**(1), 1–22 (1990).
58. E. A. Salegio et al., "Axonal transport of adeno-associated viral vectors is serotype-dependent," *Gene Ther.* **20**(3), 348–352 (2013).
59. C. Towne et al., "Neuroprotection by gene therapy targeting mutant SOD1 in individual pools of motor neurons does not translate into therapeutic benefit in fALS mice," *Mol. Ther.* **19**(2), 274–283 (2011).
60. S. J. Zhang et al., "Optogenetic dissection of entorhinal-hippocampal functional connectivity," *Science* **340**(6128), 1232627 (2013).
61. J. G. Malpeli and F. H. Baker, "The representation of the visual field in the lateral geniculate nucleus of Macaca mulatta," *J. Comp. Neurol.* **161**(4), 569–594 (1975).
62. A. Asokan, D. V. Schaffer, and R. J. Samulski, "The AAV vector toolkit: poised at the clinical crossroads," *Mol. Ther.* **20**(4), 699–708 (2012).

63. M. A. Colle et al., "Efficient intracerebral delivery of AAV5 vector encoding human ARSA in non-human primate," *Hum. Mol. Genet.* **19**(1), 147–158 (2009).
64. H. Chen et al., "Oligodendrocyte-specific gene expression in mouse brain: use of a myelin-forming cell type-specific promoter in an adeno-associated virus," *J. Neurosci. Res.* **55**(4), 504–513 (1999).
65. S. Gholizadeh et al., "Transduction of the central nervous system after intracerebroventricular injection of adeno-associated viral vectors in neonatal and juvenile mice," *Hum. Gene Ther. Methods* **24**(4), 205–213 (2013).
66. T. J. McCown et al., "Differential and persistent expression patterns of CNS gene transfer by an adeno-associated virus (AAV) vector," *Brain Res.* **713**(1–2), 99–107 (1996).
67. I. Gruh et al., "Human CMV immediate-early enhancer: a useful tool to enhance cell-type-specific expression from lentiviral vectors," *J. Gene Med.* **10**(1), 21–32 (2008).
68. B. H. Liu et al., "CMV enhancer/human PDGF-beta promoter for neuron-specific transgene expression," *Gene Ther.* **11**(1), 52–60 (2004).
69. D. L. Benson et al., "Differential effects of monocular deprivation on glutamic acid decarboxylase and type II calcium-calmodulin-dependent protein kinase gene expression in the adult monkey visual cortex," *J. Neurosci.* **11**(1), 31–47 (1991).
70. X. B. Liu and E. G. Jones, "Localization of alpha type II calcium calmodulin-dependent protein kinase at glutamatergic but not gamma-aminobutyric acid (GABAergic) synapses in thalamus and cerebral cortex," *Proc. Natl. Acad. Sci.* **93**(14), 7332–7336 (1996).
71. B. Tighilet, T. Hashikawa, and E. G. Jones, "Cell- and lamina-specific expression and activity-dependent regulation of type II calcium/calmodulin-dependent protein kinase isoforms in monkey visual cortex," *J. Neurosci.* **18**(6), 2129–2146 (1998).
72. A. M. Aravanis et al., "An optical neural interface: in vivo control of rodent motor cortex with integrated fiberoptic and optogenetic technology," *J. Neural Eng.* **4**(3), S143–S156 (2007).
73. J. L. Nathanson et al., "Short promoters in viral vectors drive selective expression in mammalian inhibitory neurons, but do not restrict activity to specific inhibitory cell-types," *Front. Neural Circuits* **3**, 19 (2009).
74. K. Low, P. Aebischer, and B. L. Schneider, "Direct and retrograde transduction of nigral neurons with AAV6, 8, and 9 and intraneuronal persistence of viral particles," *Hum. Gene Ther.* **24**(6), 613–629 (2013).
75. W. San Sebastian et al., "Adeno-associated virus type 6 is retrogradely transported in the non-human primate brain," *Gene Ther.* **20**(12), 1178–1183 (2013).
76. J. M. Alisky et al., "Transduction of murine cerebellar neurons with recombinant FIV and AAV5 vectors," *NeuroReport* **11**(12), 2669–2673 (2000).
77. D. F. Aschauer, S. Kreuz, and S. Rumpel, "Analysis of transduction efficiency, tropism and axonal transport of AAV serotypes 1, 2, 5, 6, 8 and 9 in the mouse brain," *PLoS One* **8**(9), e76310 (2013).
78. J. C. Paterna, J. Feldon, and H. Bueler, "Transduction profiles of recombinant adeno-associated virus vectors derived from serotypes 2 and 5 in the nigrostriatal system of rats," *J. Virol.* **78**(13), 6808–6817 (2004).
79. M. Rothermel et al., "Transgene expression in target-defined neuron populations mediated by retrograde infection with adeno-associated viral vectors," *J. Neurosci.* **33**(38), 15195–15206 (2013).
80. S. M. Sherman and R. W. Guillery, "Functional organization of thalamocortical relays," *J. Neurophysiol.* **76**(3), 1367–1395 (1996).
81. C. S. Peden et al., "Striatal readministration of rAAV vectors reveals an immune response against AAV2 capsids that can be circumvented," *Mol. Ther.* **17**(3), 524–537 (2009).

Annelies Gerits obtained her PhD from the laboratory of neuro- and psychophysiology at the KU Leuven and then worked as a postdoctoral fellow at the Martinos Imaging Center affiliated with the Harvard Medical School. She is now a postdoctoral fellow of the FWO Vlaanderen and working again in the laboratory of neuro- and psychophsyiology of Wim Vanduffel.

Pascaline Vancraeyenest obtained her MA at the biomedical sciences department of KU Leuven. She conducted her master's thesis under the supervision of Wim Vanduffel and Annelies Gerits in the laboratory of neuro- and psychophysiology. Her master's thesis was nominated second-best of her graduating year. She is now a doctoral fellow of the IWT Vlaanderen and is still working in the laboratory of Wim Vanduffel.

Samme Vreysen obtained his master's degree in biochemistry and biotechnology at KU Leuven and is working towards a PhD in the laboratory of neuroplasticity and neuroproteomics of Lutgarde Arckens.

Marie-Eve Laramée obtained her PhD in cellular and molecuar biology (neurosciences) from the Université du Québec à Trois-Rivières under the supervision of Denis Boire. She is now a postdoctoral fellow (FRQS fellowship) at KU Leuven in the laboratory of neuroplasticity and neuroproteomics of Lutgarde Arckens.

Annelies Michiels received a PhD in medical sciences at the Vrije Universiteit Brussel, Belgium, in 2006. In November 2006, she was appointed as a medical information manager at Ismar Healthcare, Belgium. At the end of 2009, she joined the Laboratory of Neurobiology and Gene Therapy of the KU Leuven as an Industrial Research Manager and has been managing the Leuven Viral Vector Core (LVVC) and the Neuro Drug Discovery platform.

Rik Gijsbers has been trained as a bioscience-engineer, and obtained his PhD in medical sciences at KU Leuven and remained at UPenn School of Medicine, Philadelphia, as a postdoctoral fellow. He studies viral vector integration and set up a viral vector core at the KU Leuven, where he now heads a research group developing safer vectors for gene therapy.

Chris Van den Haute studied biology at KU Leuven and obtained his PhD at the laboratory for Experimental Genetics and Transgenesis. In 2002, he joined the Laboratory for Neurobiology and Gene Therapy at KU Leuven under the supervision of Prof. Veerle Baekelandt. Since 2010, he has had a position as research expert in this group.

Lieve Moons obtained her PhD in science at KU Leuven. She worked as a postdoctoral fellow and group leader in the Vesalius Research Center (previously Center for Transgene Technology and Gene Therapy, VIB & KU Leuven). Since 2008, she has been a full professor in the biology department of KU Leuven and head of the neural circuit development and regeneration research group, which focuses on defining molecular mechanisms underlying neurodegeneration, neuroinflammation and regeneration in the visual system.

Zeger Debyser received his MD in 1990 and his PhD in 1994, both from KU Leuven in Belgium. He was a postdoctoral fellow at Harvard Medical School, USA, from 1992 to 1993. In 2000, he was appointed to the faculty of KU Leuven. Since 2009, he has been a full professor at KU Leuven. He has authored over 200 scientific publications and multiple patents. His scientific interests are molecular virology, drug discovery, and gene therapy.

Veerle Baekelandt obtained her PhD in biology in 1995 at KU Leuven and then did postdoctoral work at the faculty of medicine. She now has her own research group (Laboratory for Neurobiology and Gene Therapy at the Department of Neurosciences), focusing on familial forms of Parkinson's disease and adult neurogenesis using viral vector technology, stereotactic neurosurgery, and noninvasive molecular imaging as core technologies.

Lutgarde Arckens obtained her PhD from the laboratory of neuroplasticity and neuroproteomics at KU Leuven and then worked as a postdoctoral fellow in the same laboratory. Since October 2003, she has been a full professor at KU Leuven and is the head of the research group of neuroplasticity and neuroproteomics focusing on the molecular and structural mechanisms of plasticity in mammalian cortex.

Wim Vanduffel obtained his PhD from the laboratory of neuro- and psychophysiology at the KU Leuven and then worked as a postdoctoral fellow in the same laboratory. Afterwards, he served as instructor to the Martinos Center for Biomedical Imaging of the Massachusetts General Hospital, becoming an assistant professor at Harvard Medical School. He is also currently a full professor at KU Leuven and serves as administrative head of the lab of neuro-and psychophysiolgy.